of prostaglandin E2 production [7] and inhibition of phospholipase A2 (PLA2) [8].

Many anti-viral effects of GL have been reported previously, for example, against herpes simplex type 1 (HSV-1) [9], varicella-zoster virus (VZV) [10], hepatitis A (HAV) [11] and B virus (HBV) [12], human immunodeficiency virus (HIV) [13], severe acute respiratory syndrome (SARS) and coronavirus [14], Epstein–Barr virus (EBV) [15], human cytomegalovirus [16] and influenza virus [17]. GL has been considered as a potential treatment for patients with chronic hepatitis C, and long term administration of GL to patients is effective in suppressing serum alanine aminotransferase (ALT) levels and histological change [18]. However, a direct anti-viral effect of GL against HCV has never been reported.

In this study, we evaluated the anti-HCV effects of GL, and demonstrated that GL targeted the release step of infectious HCV particles from infected cells. We found that the suppression of virus release by GL may be derived from its inhibitory effect on group 1B PLA2 (PLA2G1B). These findings suggest possible novel roles for GL in the treatment of patients with chronic hepatitis C.

Materials and Methods

Cell culture and reagents

The human hepatoma cell line, Huh7, and its derivative cell line, Huh7.5.1, provided by Francis Chisari (Scripps Research Institute, La Jolla, CA), were maintained in Dulbecco's modified Eagle's medium (DMEM) containing 10% fetal bovine serum (FBS) [19]. Huh7 cells harboring the subgenomic replicon [20] [21] were maintained in complete DMEM supplemented with 0.5 mg/ml G418 (Geneticin, Life Technologies Japan Ltd., Tokyo, Japan). GL (20β-carboxyl-11-oxo-30-norolean-12-en-3β-yl-2-O-β-D-glucopyranuronosyl-β-D-glucopyranosiduronic acid) and IFN-α were kindly provided by the Minophagen Pharmaceutical Co., Ltd., (Tokyo, Japan) and MSD K.K., (Tokyo, Japan) respectively. Oleyloxyethyl phosphorylcholine (OPC) (Cayman Chemical Company, Ann Arbor, MI), sPLA2IIA Inhibitor I (MERCK, Darmstadt, Germany), anti-Actin (Santa Cruz Biotechnology, Santa Cruz, CA) and anti-Human CD81 (BD Pharmingen, San Jose, CA) antibodies were purchased. The solvents were distilled water (GL), ethanol (OPC), and DMSO (sPLA2IIA inhibitor).

Quantification of HCV core antigen and cell viability

The production of cell culture-produced HCV (HCVcc) has been previously reported [22]. Purification of LD has been previously reported [23]. The concentration of HCV core antigen in filtered culture medium, in cell lysates and in LD fraction of infected cells was determined using the Lumipulse Ortho HCV antigen kit (Ortho Clinical Diagnostics, Tokyo, Japan). Cell viability was analyzed by using Cell Titer-Glo Luminescent Cell Viability Assay (Promega, Madison, WI) according to the manufacturers' protocol.

Electroporation of HCV RNA lacking E1 and E2

In vitro synthesis of HCV RNA JFH1 lacking E1 and E2 (JFH1delE1E2), and electroporation were performed as described previously [22].

HCV pseudoparticle (HCVpp) assay

HCVpp harboring E1 and E2 glycoproteins of the JFH-1 clone (genotype 2a) (HCVpp2a) and the TH clone (genotype 1b) (HCVpp1b) were produced as previously described [24]. Pseudotype virus with VSV G glycoprotein (VSVpp) were also generated [24]. Huh7 or Huh7.5.1 cells were seeded into 48-well plates, incubated overnight at 37°C, and then infected with the HCVpp in the presence of various concentration of GL. Several hours post-infection, medium was replaced with DMEM with 10% FBS, and the cells were harvested 48 hours later to determine intracellular luciferase activity (Luciferase Assay System, Promega).

HCV subgenomic replicon assay

The assay for the genotype 1b and 2a subgenomic reporter replicon has been previously reported [20] [21]. After 72 hours of treatment with GL, the replicon-transfected cells were harvested for either measurement of luciferase activity (Promega) or HCV RNA titer, as described previously [25]. The replication efficiency of HCV in each preparation was calculated as the percentage of luciferase activity or HCV RNA titer compared with that of cells subjected to the control treatment.

Extra- and intracellular infectivity

To determine extracellular HCV infectivity, naïve Huh7 cells were inoculated with cell culture supernatant medium containing HCVcc. After 3 hours of incubation, the medium was replaced with DMEM containing 10% FBS, and the cells were cultured for an additional 72 hours. The infectious HCV titer in the culture medium was determined by quantification using the Lumipulse Ortho HCV antigen kit or by immunostaining of the HCV core antigen. Using an immunoassay that also provided results indicative of HCV infectivity [26], we confirmed a good correlation between the levels of core antigen and infectious titers (data not shown). To estimate intracellular infectivity, cells in the culture plates filled with DMEM containing 10% FBS were subjected to four cycles of freezing and thawing, using dry ice and a 37°C water bath. Cells in the culture plates were centrifuged at 1,200 rpm for 5 min at 4°C to remove cell debris, and the supernatants were collected to evaluate infectivity as above.

RNA interference

The siRNA targeted to PLA2G1B, 5'-GCUGGACAGCUGUAAAUUUTT-3', and scramble negative control siRNA to PLA2G1B were purchased from Sigma (Tokyo, Japan). Cells in a 24-well plate were transfected with siRNA using HiPerFect transfection reagent (Qiagen, Tokyo, Japan) following the manufacturer's instructions.

Quantification of triglyceride

Triglyceride (TG) was measured with a Triglyceride kit (Wako, Tokyo, Japan) according to the manufacturer's instructions.

Indirect immunofluorescence assay

The inoculated cells were fixed with methanol and immunostained with a mouse monoclonal anti-core antibody and a rabbit polyclonal anti-NS5A antibody [22], followed by an Alexa Fluor 555-conjugated anti-mouse secondary antibody (Life Technologies Japan Ltd.).

Transmission electron microscopy (EM)

Cells were fixed with 1.5% glutaraldehyde in 1.0% cacodylate buffer, pH 7.4, for 5 min, and then post-fixed with 2% OsO_4 in phosphate buffer, pH 7.4, for 1 hour. The cells were dehydrated in ethanol and embedded in Epon. Ultrathin sections were double stained and examined at an accelerating voltage of 80 keV. Immuno-EM (IEM) were performed by using the labeled-(strept) avidin-biotin (LAB) kit according to the manufacturer's instructions (Zymed laboratories, San Francisco, CA) as described previously [27].

Statistical Analysis

Assays were performed at least four independent experiments. Data are expressed as the mean ± SD. Statistical analysis was performed using Student's t test.

Results

Anti-HCV effects of GL

To assess the anti-HCV effects of GL, HCVcc-infected cells were treated with various concentrations of GL for 72 hours, and then the levels of HCV core antigen and infectivity of the medium were determined. HCV core antigen levels were reduced by 29% with 500 μM GL (Figure S1). As shown in Figure 1A, infectivity of supernatant following GL treatment at 3, 30, or 500 μM was reduced by 12, 62, or 71% of the control levels, respectively. The calculated 50% effective concentration (EC_{50}) was 16.5 μM. There was no effect on cell viability after these treatments (Figure 1B). These results suggest that GL effectively inhibited the production of infectious HCV.

HCV propagates in hepatocytes throughout its lifecycle, including the stages of attachment, entry, uncoating, translation, genome replication, assembly, budding, and release. To investigate which step of the HCV lifecycle GL inhibited, we used the HCVpp system for evaluating attachment and entry, and the HCV replicon system for translation and genome replication. Treatment of HCVpp2a with GL resulted in a moderate reduction of luciferase activity in the cells infected with HCVpp, with an EC_{50} value of 728 μM (Figure 1C). On the other hand, there was no significant reduction of luciferase activity in the cells infected with HCVpp1b (Figure 1D) and VSVpp (Figure 1E). No cytotoxic effects of GL were observed (data not shown).

Huh7 cells harboring the type-2a subgenomic replicon were treated with various concentrations of GL for 72 hours. Relative luciferase activities of GL-treated cells were inhibited in a dose-dependent manner with an EC_{50} value of 738 μM (Figure 1F). A similar result was obtained by using the type-1b subgenomic replicon (data not shown). We also transfected HCV RNA lacking E1E2 (JFH1delE1E2) and monitored the effect of GL on HCV replication to avoid reinfection of Huh7 cells. There was no significant reduction of HCV RNA titers in the cells (Figure 1G). There was no significant cytotoxicity seen following these treatments (data not shown).

To investigate the effect of GL on entry, HCV particles were treated with increasing concentrations (0 to 1500μM) of GL. The viral samples were then used to inoculate Huh7 cells cultured in GL-containing medium. Several hours post-infection, medium was replaced with DMEM without GL. The levels of HCV core antigen in the medium were determined at 72 h postinfection (p.i.). There was no significant reduction of HCV production (Figure 1H). These results indicated that GL did not inhibited HCV entry and replication significantly.

Effects of GL on infectious HCV particle release

To further assess whether GL treatment affects other steps of the viral lifecycle, we analyzed infectious HCV particle assembly and release following GL treatment. Supernatant or crude cell lysates of HCVcc-infected cells treated with GL were used to inoculate naïve Huh7 cells to determine extra- and intracellular specific infectivity, respectively. Specific infectivity was determined as the ratio of infectious virus titer to HCV core antigen level, as described previously [28]. As shown in Figure 2A, the extracellular specific infectivity titer was inhibited by 57% by GL at a concentration of 500 μM, on the other hand, the intracellular specific infectivity titer was increased 3.8-fold over that of controls at the same concentration of GL (Figure 2B). There was no significant cytotoxicity following these treatments (data not shown).

It has been previously reported that virus assembly takes place around lipid droplets (LDs) [29]. By immunofluorescence staining, we examined the subcellular co-localization of HCV core (Figure 2C) or NS5A (Figure 2D) with LDs in HCVcc-infected cells with or without GL treatment. Un-infected cells were shown in Figure 2E. We observed HCV proteins colocalized with LDs (Figure 2C and 2D). Intensity profiles along the line segments, shown on the bottom of the images, demonstrated that core proteins were tightly colocalized with LD in the HCVcc-infected cells treated with GL, when compared with untreated cells (Figure 2C lower panel). We quantified the size of LDs in HCV-infected cells (Figure 2D) and un-infected cells (Figure 2E) with GL-treatment. We found that GL did not affect the size of LDs in un-infected cells (Figure 2F right panel). On the other hand, the size of LDs increased in HCV-infected cells with GL-treatment (Figure 2F left panel).

HCVcc-infected cells (Figure 2G) and un-infected cells (Figure 2H), treated with GL, were prepared for EM analysis. In the cytoplasm of HCV-infected cells, we observed increased numbers of LDs in close proximity to endoplasmic reticulum (ER) and the electron-dense signals on ER attached to LD (Figure 2G upper panel), which are thought to act as platforms for the assembly of viral components [29]. Interestingly, in the cytoplasm of HCV-infected cells after treatment with GL, accumulated electron-dense particles were observed on ER attached to LD (Figure 2G lower panel). IEM experiments showed that anti-core antibody stained the membrane around LDs (Figure 2I lower panel). In naïve Huh7 cells, the close association of LDs with ER was rarely observed (Figure 2H).

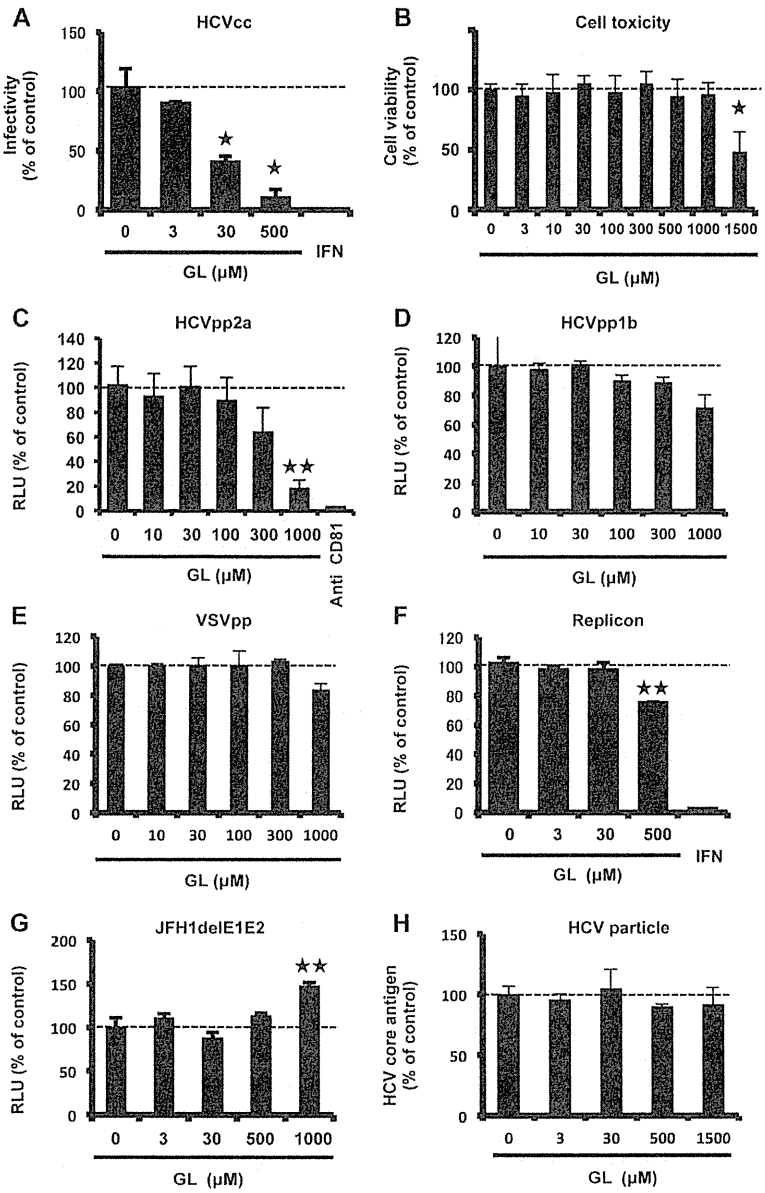

Figure 1. Anti-HCV effects of GL. (A) HCVcc-infected cells were treated with various concentrations of GL for 72 hours. Naïve Huh7 cells were inoculated with supernatant and cultured for 72 hours. Infectivity was determined by immunostaining. (B) Cell viability was assessed using Cell Titer-Glo Luminescent Cell Viability Assay. Huh7 cells were infected with HCVpp2a (C), HCVpp1b (D), and VSVpp (E) in various concentrations of GL for 24 hours, and then medium was replaced. Effects of GL on entry of HCVpp and VSVpp were determined by measuring the luciferase activity at 72 hours post-transfection. (F) Huh7 cells harboring the type-2a subgenomic replicon were treated with various concentrations of GL for 72 hours. Replication efficiency of the replicon was estimated by measuring the luciferase activity. (G) The effects of GL on HCV replication were tested by electroporation of HCV RNA lacking E1E2 (JFH1delE1E2). (H) HCV particles were treated with increasing concentrations (0 to 1500μM) of GL. The viral samples were then used to inoculate Huh7 cells with GL-containing medium. Several hours post-infection, medium was replaced with DMEM without GL. The levels of HCV core antigen of the medium were determined at 72 h postinfection (p.i.). IFN (300 IU/ml) was used as a positive control for reduced HCV replication. Anti-human CD81 antibody (10 μg/ml) was used as a positive control for reduced HCV entry to the cells. Results are expressed as the mean ± SD of the percent of the control from four independent experiments. *P < 0.05, **P < 0.005 versus control (0 μM treatment).

doi: 10.1371/journal.pone.0068992.g001

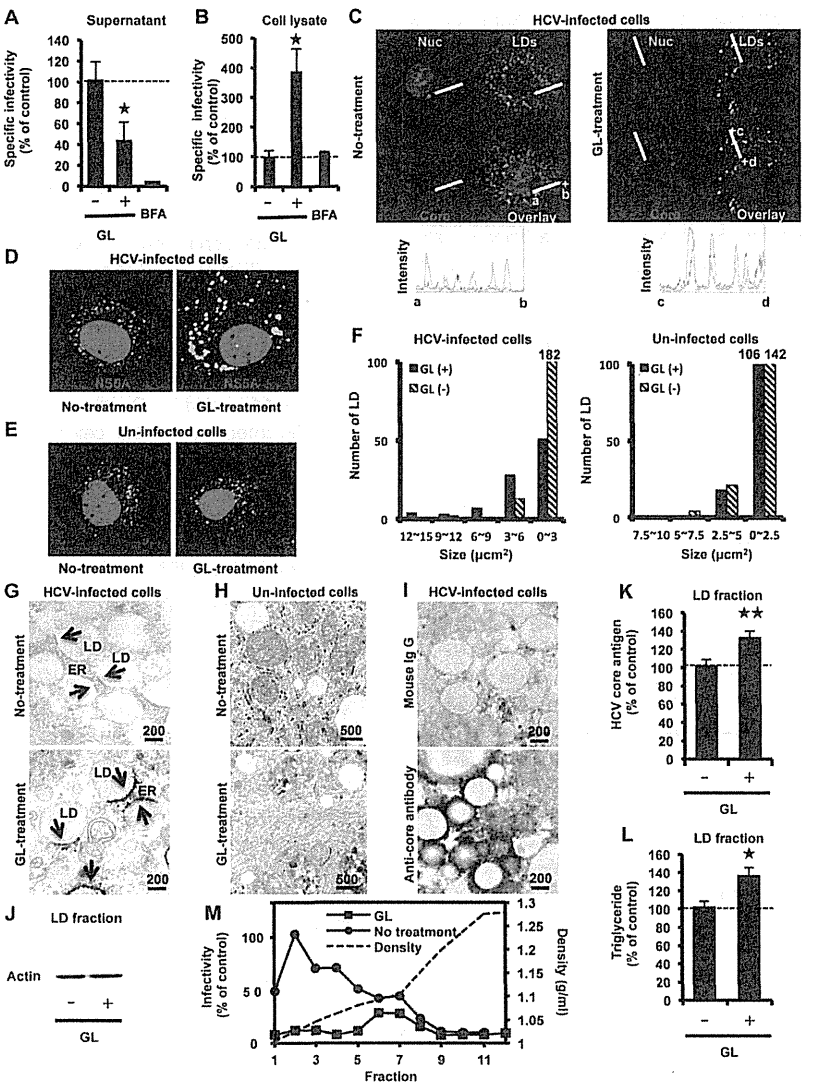

Figure 2. Effects of GL in release of infectious HCV particles. HCVcc-infected cells were treated with GL at a concentration of 500 μM for 72 hours. Untreated cells were used as controls. Extra- (A) and intracellular specific infectivity (B) were determined. Subcellular co-localization of HCV core (C) or NS5A (D) with LDs in HCVcc-infected cells with or without GL treatment. (E) Un-infected cells. LDs and nuclei were stained with BODYPI 493/503 (green) and DAPI (blue), respectively. (C) Points a and b, as well as c and d, define two line segments that each cross several structures. Intensity profiles along the line segments shown on the bottom of the images. (F) The size of LDs in un-ifected cells (right panel) and HCV-infected cells (left panel) were quantified. Transmission EM of LDs in infected cells (G) and un-infected cells (H) treated with GL at 500 μM. Arrows indicate electron-dense signals (G upper panel) and particles (G lower panel). (I) IEM using the LAB method of LDs in infected cells treated with GL at 500 μM. Mouse IgG (upper panel) or anti-core monoclonal antibody (lower panel) was used for primary antibody. (J) Immunoblotting with anti-actin antibody in the LD fraction. Quantification of HCV core antigen (K) and TG (L) in the LD fraction. The LD fraction was collected from cell lysates. The ratio of HCV core antigen level in the LD fraction to that in total cell lysate was determined. (M) HCVcc-infected cells were treated with GL at 500 μM for 72 hours. Untreated cells were used as controls. Supernatant was ultracentrifuged through a 10-60% sucrose gradient and the infectivity of each fraction was determined. Infectivity of fraction 2 of untreated cells was assigned the arbitrary value of 100%. The density of each fraction was measured by refractive index measurement. Brefeldin A (1 μM for 24 hours) was used as a positive control for reduced HCV release. Results are expressed as the mean ± SD of the percent of the control from four independent experiments. *P < 0.05, **P < 0.005 versus control (0 μM treatment). Scale bars, 200 and 500 nm.

doi: 10.1371/journal.pone.0068992.g002

To confirm the accumulation of core antigen around LD, we purified the LD [23], and quantified HCV core antigen and TG in the LD fraction, followed by immunoblotting with anti-actin antibody (Figure 2J). Analysis of the levels of HCV core antigen and TG in the LD fraction of the total cell lysate showed that the amount in GL-treated cells was increased by 31% and 35% compared with controls, respectively (Figure 2K and 2L). Taken together, these results suggested that GL inhibits release, but not assembly and budding, of infectious HCV particles in cells.

To characterize the infectivity of HCV particles released from HCVcc-infected cells treated with GL, supernatant from cell cultures treated or not treated with GL was subjected to continuous 10-60% (w/v) sucrose density gradient centrifugation, and the infectivity titer of each fraction was measured. A reduction in infectivity by GL-treatment was observed in fractions 1-7 (Figure 2M). These results suggest that GL may decrease the amount of HCV infectious particles in the supernatant.

Role of PLA2 in HCV lifecycle

GL is known to have an inhibitory effect on PLA2 [8]. PLA2 is classified into several groups and their biological functions are not the same. It is unknown which group of PLA2 is targeted by GL. We analyzed the effect of GL on PLA2G1B and PLA2G2A, which were major groups of PLA2 family. To confirm the effects of GL on expression of PLA2G1B, cells, transfected with an expression plasmid for PLA2G1B, were treated with GL and OPC, which is a specific inhibitor for PLA2G1B. Treatment with GL effectively decreased the cellular level of PLA2G1B (Figure S2). To verify whether PLA2 has a role in viral entry and replication, we tested the effect of PLA2 inhibitors on HCVpp infection and the replicon system, respectively. OPC has no significant effect on virus entry and replication (Figure 3A and 3B). On the other hand, sPLA2IIA inhibitor I, which is a specific inhibitor for PLA2G2A, inhibited both HCVpp entry (Figure 3A) and subgenomic replicon replication (Figure 3B). There was no significant cytotoxicity seen after these treatments (data not shown).

To evaluate the effects of PLA2 inhibitors on HCVcc infectivity, infected cells were treated with PLA2 inhibitors and extra- and intracellular specific infectivity were measured (Figure 3C and 3D). OPC slightly decreased specific infectivity of virus in the supernatant and significantly increased specific infectivity of virus in the cell lysate. On the other hand, sPLA2IIA inhibitor I significantly decreased the specific infectivity of virus in both the supernatant and cell lysate. To confirm the importance of PLA2G1B in HCV release, we silenced PLA2G1B with its specific siRNA and monitored its effect on HCV release. PLA2G1B siRNA decreased the cellular level of PLA2G1B (Figure S3). Suppression of PL2G1B reduced core protein level in the medium (Figure 3E left panel) and increased specific infectivity in the cells (Figure 3E right panel). We performed GL treatment with or without OPC and showed that GL and OPC had no additive effect when applied together (Figure 3F). There was no significant cytotoxicity seen after these treatments (data not shown). Taken together, these results suggest that the suppression of virus release by GL may be derived from its inhibitory effect on PLA2G1B. These results also suggested that PLA2G1B has a role in virus release.

Antiviral effects of IFN along with GL

We have demonstrated that the target causing the anti-HCV effect of GL differs from that of IFN. To analyze the antiviral effect of IFN combined with GL, HCVcc-infected cells were treated with 0.1 and 1.0 IU/ml of IFN in combination with various concentrations of GL. HCV core level in culture medium (Figure 4A) and in the cell (Figure 4B), specific infectivity in culture medium (Figure 4C) and in the cells (Figure 4D) were measured. Regardless to the IFN concentration, HCV core level and specific infectivity of the supernatant decreased in response to GL treatment in a dose dependent manner (Figure 4A and 4C). On the other hand, HCV core level and specific infectivity of the cell increased (Figure 4B and 4D), suggesting that GL inhibited HCV release. The results indicated that a combination therapy of IFN with GL could be an effective treatment for HCV.

Effect of GL on IFN induction and secretion proteins

The IFN-inducing ability of GL has also been previously reported [30]. We evaluated IFN stimulated gene induction by GL, but no effects were observed (Figure S4). PLA2 is known to be associated with various intracellular trafficking events and secretion of very low-density lipoprotein (VLDL) [31]. HCV particles are known to be secreted using the host membrane trafficking system [32]. There is now increasing evidence that VLDL participates in HCV assembly and release [33]. Therefore, we analyzed the level of albumin, an abundantly secreted protein from hepatocytes, and apolipoprotein E (ApoE), a component of lipoproteins, in the culture supernatants of Huh7 cells and found that they were not influenced by GL treatment (Figure S5).

Discussion

Recently, Ashfaq et al. found the inhibitory effect of GL on HCV production in patient serum infected Huh7 cells [34]. Their cell culture system does not produce HCV efficiently. Thus, it does not permit analysis of the complete viral life cycle. In this study, we observed distinct suppression of HCV release by GL, using the HCVcc system (Figure 1A). Anti-viral effects of GL on early steps in the viral lifecycle have been reported previously, for example the inhibition of endocytosis of influenza A virus (IAV), the direct fusion of HIV-1 [35], the penetration of the plasma membrane of HAV [11] and EBV [15], the virus entry of SARS [14], and infection by pseudorabies virus [36]. GL effectively inhibits the replication of VZV [10], HSV-1 [9], EBV [15] and HIV [13]. This is the first report that GL can suppress virus release, however, the detailed mechanisms of these remain elusive. It has also been reported that GL had a membrane stabilizing effect [37] and a reduction of membrane fluidity [35], [38]. HCV uses cellular membrane structure in its lifecycle [39], [40]. Thus, it is conceivable that membrane alterations may play a negative role in the HCV lifecycle.

We found core protein accumulation on LDs in GL-treated cell (Figure 2C, 2I and 2K). This inverse correlation between

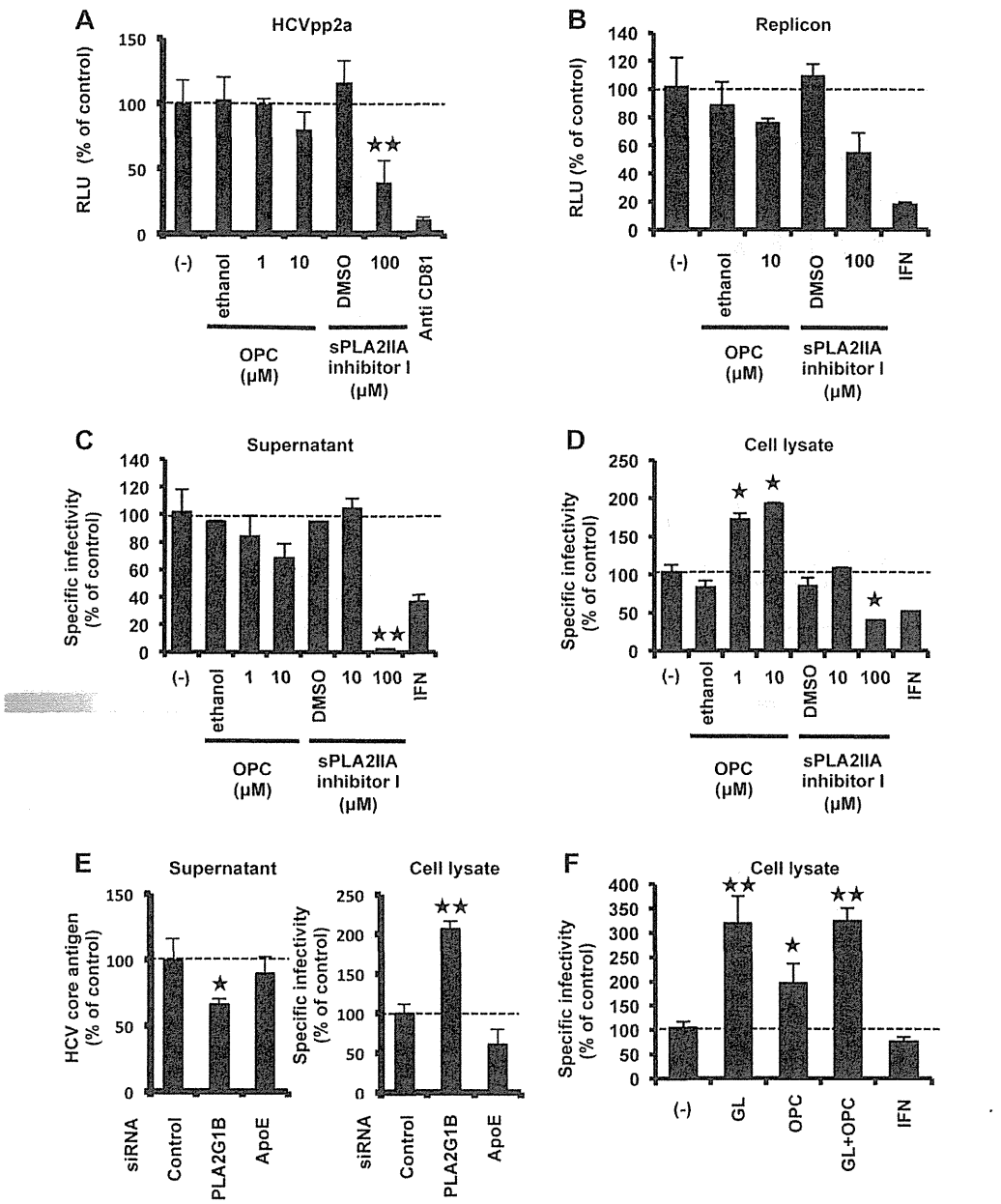

Figure 3. A role of PLA2 in HCV lifecycle. (A) Huh7 cells were infected with HCVpp in the presence and absence of OPC or sPLA2IIA inhibitor for 2 hours, then medium was replaced. Effects of PLA2 inhibitor on the entry of HCVpp were determined by measuring the luciferase activity at 72 hours post-infection. Anti-human CD81 antibody (10 μg/ml) was used as a positive control for reducing HCV entry to the cells. (B) Huh7 cells harboring the type-2a subgenomic replicon were treated with OPC or sPLA2IIA inhibitor for 72 hours. Replication efficiency of the replicon was estimated by measuring HCV RNA titer. HCVcc-infected cells were treated with PLA2 inhibitor for 72 hours. Specific infectivity of the supernatant (C) and cell lysate (D) were evaluated by quantifying the HCV core antigen in cells at 72 hours post-infection. (E) Effects of siRNA against PLA2G1B on core level in the medium (left panel) and specific infectivity in HCV-infected cells (right panel). ApoE siRNA was used as a positive control for reduced HCV infectivity. (F) HCVcc-infected cells were treated with GL (500 μM) with or without OPC (10 μM), and intracellular specific infectivity was measured. IFN (10 IU/ml) was used as a positive control. Results are expressed as the mean ± SD of the percent of the control from four independent experiments. *P < 0.05, **P < 0.005 versus control (0 μM treatment).

doi: 10.1371/journal.pone.0068992.g003

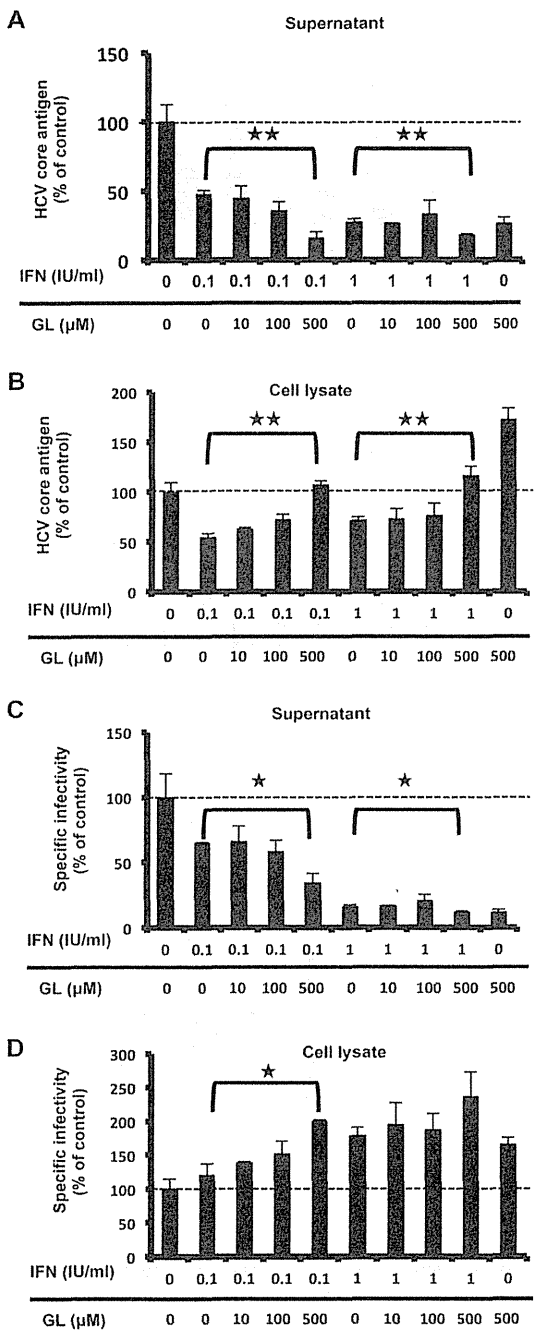

Figure 4. Anti-HCV effects IFN in combination with GL. HCVcc-infected cells were treated with IFN alone, or IFN with GL for 72 hours. HCV production was assessed by measuring the HCV core antigen in culture medium (A) and cell (B). Specific nfectivity in culture medium (C) and cell (D) were measured. Results are expressed as the mean ± SD of the percent of the control from four independent experiments. *P < 0.05, **P < 0.005 versus versus IFN mono-therapy.

doi: 10.1371/journal.pone.0068992.g004

the efficiency of virus production and core protein accumulation on LDs was also observed that colocalization of HCV protein with LDs was low in cases of the chimera Jc1, supporting up to 1,000-fold higher infectivity titers compared with JFH1 [41], [29]. In this study, we demonstrated that GL did not affect the size of LDs in un-infected cells (Figure 2F right panel). On the other hand, the size of LDs increased in HCV-infected cells with GL-treatment (Figure 2F left panel), probably because accumulated-HCV enhanced the formation of LDs [29].

We demonstrated the importance of PLA2G1B in HCV release by PLA2G1B inhibitor and siRNA against PLA2G1B (Figure 3). The overexpression of PLA2G1B did not have any effect on HCV release (data not shown), probably because enough PLA2G1B existed in the cells. This result is generally observed in other host factors that involved in HCV lifecycle. For example, overexpression of the human homologue of the 33-kDa vesicle-associated membrane protein-associated protein (hVAP-33), which has a critical role in the formation of HCV replication complex, did not increase HCV replication [42]. PLA2 family proteins have been known as lipid-signaling molecules, inducing inflammation [43]. On the basis of the nucleotide sequence, the superfamily of PLA2 enzymes consists of 15 groups, comprising 4 main types: cytosolic PLA2 (cPLA2), calcium-independent PLA2, platelet activating factor acetyl hydrolase/oxidized lipid lipoprotein associated PLA2, and the secretory PLA2 (sPLA2) including PLA2G1B, 2A, and 4A [44]. In this study, we showed that GL, PLA2G1B inhibitor, and PLA2G1B siRNA inhibited HCV release and that GL and OPC had no additive effect when applied together, suggesting that suppression of HCV release by GL may be derived from its inhibitory effect on PLA2G1B. The role of PLA2G1B in the HCV lifecycle has not been reported. In this study, we also demonstrated that PLA2G2A inhibitor decreased entry, replication, and assembly of infectious HCV particles in cells (Figures 3A, 3B, 3C, and 3D). The role of PLA2G2A in the HCV lifecycle has not been reported. PLA2G2A is known to affect the secretion of VLDL (30). Therefore, PLA2G2A may contribute to HCV assembly. In the case of PLA2G4A, Menzel et al. showed that inhibition of PLA2G4A produces aberrant HCV particles [45]. These observations suggest that PLA2 has a role in several steps of the HCV lifecycle.

In this study, we showed that the EC_{50} of GL treatment for intracellular infectivity was 16.5 μM (Figure 1A). It has been reported that the maximum peripheral concentration of GL in normal patients is 145 μM [46]. The placebo-controlled phase I/II trial revealed no significant effect on viral titer [47]. In vivo, accumulated HCV in GL treated cells may cause lysis and apoptosis of the cells, leading to the release of infectious particles in the circulation. This may be a major limitation to use GL mono-therapy against HCV infection in patients. On the other hand, combination treatment with GL augmented the IFN-induced reduction in HCV core antigen levels (Figure 4A).

Although a number of natural compounds with anti-HCV activities were identified in recent years (Silymarin, EGCG, Ladanein, Naringenin, Quercetin, Luteolin, Honokiol, 3-hydroxy caruilignan C, and other things) [48], many aspects concerning their mechanisms of action remain unknown. In this study, GL is identified as a novel anti-HCV agent that targets the release

steps of infectious HCV particles. We found that the suppression of viral release by GL may be due to an inhibitory effect of PLA2G1B. These observations provide a basis for development of an improved IFN-based combination therapy against chronic hepatitis C.

Supporting Information

Figure S1. Anti-HCV effect of GL. HCVcc-infected cells were treated with various concentrations of GL for 72 hours. HCV production was assessed by measuring the level of HCV core antigen in culture medium. Results are expressed as the mean ± SD of the percent of the control from four independent experiments. IFN (10 IU/ml) was used as a positive control. *P < 0.05, **P < 0.005 versus control (0 μM treatment).
(TIF)

Figure S2. Effect of GL on expression of PLA2G1B. A human PLA2G1B cDNA was inserted into the EcoRI site of pCAGGS, yielding pCAGPLA2G1B. Since there was no effective antibody to detect endogenous expression of PLA2G1B, 293T cells transfected with the pCAGPLA2G1B plasmid were treated with GL (500 μM) for 72 hours and lysed in lysis buffer, followed by immunoblotting with anti-PLA2G1B and anti-actin antibodies. OPC (10 μM) was used as a positive control to reduce PLA2G1B protein in the cells.
(TIF)

Figure S3. Effect of PLA2G1B siRNA on expression of PLA2G1B. HCVcc infected-Huh7 cells in a 24-well plate were transfected with siRNAs targeted to PLA2G1B and scramble negative control siRNA, followed by immunoblotting with anti-PLA2G1B and anti-actin antibodies.
(TIF)

Figure S4. Effect of GL on IFN induction. The pISRE-Luc vector contains the firefly luciferase reporter gene, downstream of the IFN-Stimulated Response Element (ISRE) cis-acting enhancer element. The pRL-TK vector contains the renilla luciferase reporter downstream of the herpes simplex virus thymidine kinase (HSV-TK promoter), and was used as an internal control. Huh7 cells transfected with the pISRE-Luc vector and the pRL-TK vector were treated with various concentrations of GL for 72 hours, and luciferase activities were measured using the Dual-Luciferase Reporter Assay System. IFN (300 U/ml) was used as a positive control. Results are expressed as the mean ± SD percent of the controls (treatment with IFN).
(TIF)

Figure S5. Effect of GL on secretion of lipoprotein and the host proteins. Huh7 cells were treated or untreated with GL at 500 μM for 72 hours. ApoE and albumin in the culture supernatants were measured by immunoblotting and ELISA, respectively. Results are expressed as the mean ± SD of the percent of the control from four independent experiments.
(TIF)

Acknowledgements

We are grateful to Francis V. Chisari (Scripps Research Institute) for Huh7.5.1 cells. We thank M. Sasaki for technical assistance and T. Mizoguchi for secretarial assistance.

Author Contributions

Conceived and designed the experiments: YM NW RS SI TS T. Miyamura T. Matsuura TW SH K. Wake K. Watashi. Performed the experiments: YM H. Aoyagi H. Aizaki. Analyzed the data: YM H. Aoyagi H. Aizaki. Contributed reagents/materials/analysis tools: MM TD. Wrote the manuscript: YM H. Aoyagi.

References

1. Manns MP, McHutchison JG, Gordon SC, Rustgi VK, Shiffman M et al. (2001) Peginterferon alfa-2b plus ribavirin compared with interferon alfa-2b plus ribavirin for initial treatment of chronic hepatitis C: a randomised trial. Lancet 358: 958-965. doi:10.1016/S0140-6736(01)06102-5. PubMed: 11583749.
2. Fujisawa Y, Sakamoto M, Matsushita M, Fujita T, Nishioka K (2000) Glycyrrhizin inhibits the lytic pathway of complement--possible mechanism of its anti-inflammatory effect on liver cells in viral hepatitis. Microbiol Immunol 44: 799-804. PubMed: 11092245.
3. Hibasami H, Iwase H, Yoshioka K, Takahashi H (2006) Glycyrrhetic acid (a metabolic substance and aglycon of glycyrrhizin) induces apoptosis in human hepatoma, promyelotic leukemia and stomach cancer cells. Int J Mol Med 17: 215-219. PubMed: 16391818.
4. Inoue H, Mori T, Shibata S, Saito H (1987) Pharmacological activities of glycyrrhetinic acid derivatives: analgesic and anti-type IV allergic effects. Chem Pharm Bull (Tokyo) 35: 3888-3893. doi:10.1248/cpb.35.3888. PubMed: 3435983.
5. Pompei R, Flore O, Marccialis MA, Pani A, Loddo B (1979) Glycyrrhizic acid inhibits virus growth and inactivates virus particles. Nature 281: 689-690. doi:10.1038/281689a0. PubMed: 233133.
6. Francischetti IM, Monteiro RQ, Guimarães JA (1997) Identification of glycyrrhizin as a thrombin inhibitor. Biochem Biophys Res Commun 235: 259-263. doi:10.1006/bbrc.1997.6735. PubMed: 9196073.
7. Ohuchi K, Kamada Y, Levine L, Tsurufuji S (1981) Glycyrrhizin inhibits prostaglandin E2 production by activated peritoneal macrophages from rats. Prostaglandins Med 7: 457-463. doi:10.1016/0161-4630(81)90033-1. PubMed: 6798590.
8. Ohtsuki K, Abe Y, Shimoyama Y, Furuya T, Munakata H et al. (1998) Separation of phospholipase A2 in Habu snake venom by glycyrrhizin (GL)-affinity column chromatography and identification of a GL-sensitive enzyme. Biol Pharm Bull 21: 574-578. doi:10.1248/bpb.21.574. PubMed: 9657040.
9. Sekizawa T, Yanagi K, Itoyama Y (2001) Glycyrrhizin increases survival of mice with herpes simplex encephalitis. Acta Virol 45: 51-54. PubMed: 11394578.
10. Baba M, Shigeta S (1987) Antiviral activity of glycyrrhizin against varicella-zoster virus in vitro. Antiviral Res 7: 99-107. doi:10.1016/0166-3542(87)90025-8. PubMed: 3034150.
11. Crance JM, Lévêque F, Biziagos E, van Cuyck-Gandré H, Jouan A et al. (1994) Studies on mechanism of action of glycyrrhizin against hepatitis A virus replication in vitro. Antiviral Res 23: 63-76. doi:10.1016/0166-3542(94)90176-7. PubMed: 8141593.
12. Takahara T, Watanabe A, Shiraki K (1994) Effects of glycyrrhizin on hepatitis B surface antigen: a biochemical and morphological study. J Hepatol 21: 601-609. doi:10.1016/S0168-8278(94)80108-8. PubMed: 7814808.

13. Kimoto M, Kawai R, Mitsui T, Harada Y, Sato A et al. (2005) Site-specific incorporation of fluorescent probes into RNA by specific transcription using unnatural base pairs. Nucleic Acids Symp Ser (Oxf): 287-288. PubMed: 17150746.
14. Hoever G, Baltina L, Michaelis M, Kondratenko R, Tolstikov GA et al. (2005) Antiviral activity of glycyrrhizic acid derivatives against SARS-coronavirus. J Med Chem 48: 1256-1259. doi:10.1021/jm0493008. PubMed: 15715493.
15. Lin JC (2003) Mechanism of action of glycyrrhizic acid in inhibition of Epstein-Barr virus replication in vitro. Antiviral Res 59: 41-47. doi: 10.1016/S0166-3542(03)00030-5. PubMed: 12834859.
16. Harada H, Suzu S, Ito T, Okada S (2005) Selective expansion and engraftment of human CD16+ NK cells in NOD/SCID mice. Eur J Immunol 35: 3599-3609. doi:10.1002/eji.200535125. PubMed: 16304638.
17. Utsunomiya T, Kobayashi M, Pollard RB, Suzuki F (1997) Glycyrrhizin, an active component of licorice roots, reduces morbidity and mortality of mice infected with lethal doses of influenza virus. Antimicrob Agents Chemother 41: 551-556. PubMed: 9055991.
18. Manns MP, Wedemeyer H, Singer A, Khomutjanskaja N, Dienes HP et al. (2012) Glycyrrhizin in patients who failed previous interferon alpha-based therapies: biochemical and histological effects after 52 weeks. J Viral Hepat 19: 537-546. doi:10.1111/j.1365-2893.2011.01579.x. PubMed: 22762137.
19. Zhong J, Gastaminza P, Cheng G, Kapadia S, Kato T et al. (2005) Robust hepatitis C virus infection in vitro. Proc Natl Acad Sci U S A 102: 9294-9299. doi:10.1073/pnas.0503596102. PubMed: 15939869.
20. Goto K, Watashi K, Murata T, Hishiki T, Hijikata M et al. (2006) Evaluation of the anti-hepatitis C virus effects of cyclophilin inhibitors, cyclosporin A, and NIM811. Biochem Biophys Res Commun 343: 879-884. doi:10.1016/j.bbrc.2006.03.059. PubMed: 16564500.
21. Miyamoto M, Kato T, Date T, Mizokami M, Wakita T (2006) Comparison between subgenomic replicons of hepatitis C virus genotypes 2a (JFH-1) and 1b (Con1 NK5.1). Intervirology 49: 37-43. doi:10.1159/000087261. PubMed: 16166787.
22. Wakita T, Pietschmann T, Kato T, Date T, Miyamoto M et al. (2005) Production of infectious hepatitis C virus in tissue culture from a cloned viral genome. Nat Med 11: 791-796. doi:10.1038/nm1268. PubMed: 15951748.
23. Sato S, Fukasawa M, Yamakawa Y, Natsume T, Suzuki T et al. (2006) Proteomic profiling of lipid droplet proteins in hepatoma cell lines expressing hepatitis C virus core protein. J Biochem 139: 921-930. doi: 10.1093/jb/mvj104. PubMed: 16751600.
24. Akazawa D, Date T, Morikawa K, Murayama A, Miyamoto M et al. (2007) CD81 expression is important for the permissiveness of Huh7 cell clones for heterogeneous hepatitis C virus infection. J Virol 81: 5036-5045. doi:10.1128/JVI.01573-06. PubMed: 17329343.
25. Takeuchi T, Katsume A, Tanaka T, Abe A, Inoue K et al. (1999) Real-time detection system for quantification of hepatitis C virus genome. Gastroenterology 116: 636-642. doi:10.1016/S0016-5085(99)70185-X. PubMed: 10029622.
26. Koutsoudakis G, Herrmann E, Kallis S, Bartenschlager R, Pietschmann T (2007) The level of CD81 cell surface expression is a key determinant for productive entry of hepatitis C virus into host cells. J Virol 81: 588-598. doi:10.1128/JVI.01534-06. PubMed: 17079281.
27. Miyamoto Y, Kitamura N, Nakamura Y, Futamura M, Miyamoto T et al. (2011) Possible existence of lysosome-like organella within mitochondria and its role in mitochondrial quality control. PLOS ONE 6: e16054. doi:10.1371/journal.pone.0016054. PubMed: 21264221.
28. Kato T, Choi Y, Elmowalid G, Sapp RK, Barth H et al. (2008) Hepatitis C virus JFH-1 strain infection in chimpanzees is associated with low pathogenicity and emergence of an adaptive mutation. Hepatology 48: 732-740. doi:10.1002/hep.22422. PubMed: 18712792.
29. Miyanari Y, Atsuzawa K, Usuda N, Watashi K, Hishiki T et al. (2007) The lipid droplet is an important organelle for hepatitis C virus production. Nat Cell Biol 9: 1089-1097. doi:10.1038/ncb1631. PubMed: 17721513.
30. Abe N, Ebina T, Ishida N (1982) Interferon induction by glycyrrhizin and glycyrrhetinic acid in mice. Microbiol Immunol 26: 535-539. PubMed: 6290851.
31. Brown WJ, Chambers K, Doody A (2003) Phospholipase A2 (PLA2) enzymes in membrane trafficking: mediators of membrane shape and function. Traffic 4: 214-221. doi:10.1034/j.1600-0854.2003.00078.x. PubMed: 12694560.
32. Coller KE, Heaton NS, Berger KL, Cooper JD, Saunders JL et al. (2012) Molecular determinants and dynamics of hepatitis C virus secretion. PLOS Pathog 8: e1002466. PubMed: 22241992.
33. McLauchlan J (2009) Hepatitis C virus: viral proteins on the move. Biochem Soc Trans 37: 986-990. doi:10.1042/BST0370986. PubMed: 19754437.
34. Ashfaq UA, Masoud MS, Nawaz Z, Riazuddin S (2011) Glycyrrhizin as antiviral agent against Hepatitis C Virus. J Transl Med 9: 112. doi: 10.1186/1479-5876-9-112. PubMed: 21762538.
35. Harada S (2005) The broad anti-viral agent glycyrrhizin directly modulates the fluidity of plasma membrane and HIV-1 envelope. Biochem J 392: 191-199. doi:10.1042/BJ20051069. PubMed: 16053446.
36. Sui X, Yin J, Ren X (2010) Antiviral effect of diammonium glycyrrhizinate and lithium chloride on cell infection by pseudorabies herpesvirus. Antiviral Res 85: 346-353. doi:10.1016/j.antiviral.2009.10.014. PubMed: 19879899.
37. Shiki Y, Shirai K, Saito Y, Yoshida S, Mori Y et al. (1992) Effect of glycyrrhizin on lysis of hepatocyte membranes induced by anti-liver cell membrane antibody. J Gastroenterol Hepatol 7: 12-16. doi:10.1111/j.1440-1746.1992.tb00927.x. PubMed: 1543863.
38. Wolkerstorfer A, Kurz H, Bachhofner N, Szolar OH (2009) Glycyrrhizin inhibits influenza A virus uptake into the cell. Antiviral Res 83: 171-178. doi:10.1016/j.antiviral.2009.04.012. PubMed: 19416738.
39. Aizaki H, Lee KJ, Sung VM, Ishiko H, Lai MM (2004) Characterization of the hepatitis C virus RNA replication complex associated with lipid rafts. Virology 324: 450-461. doi:10.1016/j.virol.2004.03.034. PubMed: 15207630.
40. Aizaki H, Morikawa K, Fukasawa M, Hara H, Inoue Y et al. (2008) Critical role of virion-associated cholesterol and sphingolipid in hepatitis C virus infection. J Virol 82: 5715-5724. doi:10.1128/JVI.02530-07. PubMed: 18367533.
41. Pietschmann T, Kaul A, Koutsoudakis G, Shavinskaya A, Kallis S et al. (2006) Construction and characterization of infectious intragenotypic and intergenotypic hepatitis C virus chimeras. Proc Natl Acad Sci U S A 103: 7408-7413. doi:10.1073/pnas.0504877103. PubMed: 16651538.
42. Gao L, Aizaki H, He JW, Lai MM (2004) Interactions between viral nonstructural proteins and host protein hVAP-33 mediate the formation of hepatitis C virus RNA replication complex on lipid raft. J Virol 78: 3480-3488. doi:10.1128/JVI.78.7.3480-3488.2004. PubMed: 15016871.
43. Funk CD (2001) Prostaglandins and leukotrienes: advances in eicosanoid biology. Science 294: 1871-1875. doi:10.1126/science.294.5548.1871. PubMed: 11729303.
44. Burke JE, Dennis EA (2009) Phospholipase A2 structure/function, mechanism, and signaling. J Lipid Res 50 Suppl: S237-S242. PubMed: 19011112.
45. Menzel N, Fischl W, Hueging K, Bankwitz D, Frentzen A et al. (2012) MAP-Kinase Regulated Cytosolic Phospholipase A2 Activity Is Essential for Production of Infectious Hepatitis C Virus Particles. PLOS Pathog 8: e1002829. PubMed: 22911431.
46. van Rossum TG, Vulto AG, Hop WC, Schalm SW (1999) Pharmacokinetics of intravenous glycyrrhizin after single and multiple doses in patients with chronic hepatitis C infection. Clin Ther 21: 2080-2090. doi:10.1016/S0149-2918(00)87239-2. PubMed: 10645755.
47. van Rossum TG, Vulto AG, Hop WC, Schalm SW (2001) Glycyrrhizin-induced reduction of ALT in European patients with chronic hepatitis C. Am J Gastroenterol 96: 2432-2437. doi:10.1016/S0002-9270(01)02612-0. PubMed: 11513186.
48. Calland N, Dubuisson J, Rouillé Y, Séron K (2012) Hepatitis C virus and natural compounds: a new antiviral approach? Viruses 4: 2197-2217. doi:10.3390/v4102197. PubMed: 23202460.

SCIENTIFIC REPORTS

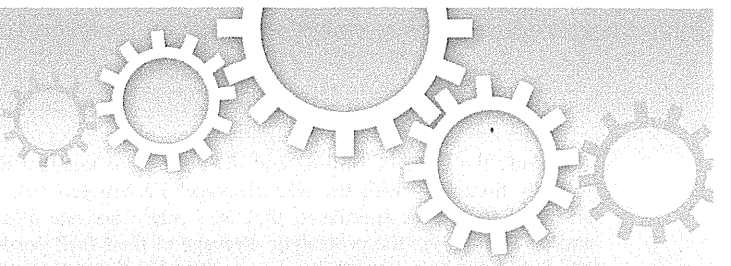

OPEN

SUBJECT AREAS:
MECHANISMS OF DISEASE
HEPATITIS C
LIVER FIBROSIS
TRANSFORMING GROWTH FACTOR BETA

Received
25 July 2013

Accepted
31 October 2013

Published
22 November 2013

Correspondence and requests for materials should be addressed to S.K. (skojima@riken.jp)

HCV NS3 protease enhances liver fibrosis via binding to and activating TGF-β type I receptor

Kotaro Sakata[1,2,3], Mitsuko Hara[1], Takaho Terada[4,5], Noriyuki Watanabe[6], Daisuke Takaya[4,7], So-ichi Yaguchi[8], Takehisa Matsumoto[4,7], Tomokazu Matsuura[9], Mikako Shirouzu[4,7], Shigeyuki Yokoyama[4,5], Tokio Yamaguchi[10], Keiji Miyazawa[8], Hideki Aizaki[6], Tetsuro Suzuki[11], Takaji Wakita[6], Masaya Imoto[2] & Soichi Kojima[1]

[1]Micro-signaling Regulation Technology Unit, RIKEN Center for Life Science Technologies, Saitama 351-0198, Japan, [2]Department of Biosciences and Informatics, Faculty of Science and Technology, Keio University, Kanagawa 223-8522, Japan, [3]Drug Discovery Laboratory, Wakunaga Pharmaceutical Co., Ltd., Hiroshima 739-1195, Japan, [4]RIKEN Systems and Structural Biology Center, Kanagawa 230-0045, Japan, [5]RIKEN Structural Biology Laboratory, Kanagawa 230-0045, Japan, [6]Department of Virology II, National Institute of Infectious Diseases, Tokyo 162-8640, Japan, [7]Division of Structural and Synthetic Biology, RIKEN Center for Life Science Technologies, Kanagawa 230-0045, Japan, [8]Department of Biochemistry, Interdisciplinary Graduate School of Medicine and Engineering, University of Yamanashi, Yamanashi 409-3898, Japan, [9]Department of Laboratory Medicine, the Jikei University School of Medicine, Tokyo 105-8461, Japan, [10]RIKEN Program for Drug Discovery and Medical Technology Platforms, Saitama 351-0198, Japan, [11]Department of Infectious Diseases, Hamamatsu University School of Medicine, Shizuoka 431-3192, Japan.

Viruses sometimes mimic host proteins and hijack the host cell machinery. Hepatitis C virus (HCV) causes liver fibrosis, a process largely mediated by the overexpression of transforming growth factor (TGF)-β and collagen, although the precise underlying mechanism is unknown. Here, we report that HCV non-structural protein 3 (NS3) protease affects the antigenicity and bioactivity of TGF-β2 in $(CAGA)_9$-Luc CCL64 cells and in human hepatic cell lines via binding to TGF-β type I receptor (TβRI). Tumor necrosis factor (TNF)-α facilitates this mechanism by increasing the colocalization of TβRI with NS3 protease on the surface of HCV-infected cells. An anti-NS3 antibody against computationally predicted binding sites for TβRI blocked the TGF-β mimetic activities of NS3 *in vitro* and attenuated liver fibrosis in HCV-infected chimeric mice. These data suggest that HCV NS3 protease mimics TGF-β2 and functions, at least in part, via directly binding to and activating TβRI, thereby enhancing liver fibrosis.

Viruses sometimes take over the host cell machinery by mimicking host cell proteins. This strategy infers survival, infection, and replication advantages to the virus[1,2], which may thereby contribute to the development of human disease.

Chronic hepatitis C virus (HCV) infection is one of the major causes of liver fibrosis, cirrhosis, and hepatocellular carcinoma[3,4]. However, the molecular mechanism by which HCV induces liver fibrosis is not fully understood. An estimated 130–170 million people worldwide are infected with HCV[5]. HCV, classified in the genus *Hepacivirus* of the family *Flaviviridae*, is a positive-strand RNA virus with an approximately 9.6-kb viral genome encoding structural (core, E1, and E2) and non-structural proteins (p7, NS2, NS3, NS4A, NS4B, NS5A, and NS5B)[6]. Of these proteins, NS3 is a member of the serine protease family that cleaves the HCV polyprotein to generate mature viral proteins that are required for viral replication[7].

Liver fibrosis, a common feature of chronic liver diseases, is caused by the excessive accumulation of extracellular matrix (ECM) proteins, including collagen. Transforming growth factor (TGF)-β, the most potent fibrogenic cytokine, is produced in its high molecular weight latent form and partly activated through the proteolytic cleavage of its propeptide region, termed latency associated protein (LAP), by serine proteases, plasmin, and plasma kallikrein[8,9]. The resultant active TGF-β signals via TGF-β type I (TβRI) and type II receptors (TβRII), inducing the phosphorylation of Smad2/3, which then binds to Smad4 and forms a complex that enters the cell nucleus. This complex acts as a transcription factor that controls the expression of target genes, including collagen and TGF-β itself, by binding to the DNA elements containing the minimal Smad-binding element, CAGA box[10].

Because the LAPs of TGF-β2 and -β3 have sequences that share partially homology with the NS3 cleavage site between NS3 and NS4A of HCV[7], we speculated that NS3 might activate TGF-β2 and/or TGF-β3 via the proteolytic cleavage of their LAP portions. We found, however, that NS3 protease DID NOT directly activate latent TGF-β2/3. Instead, it mimicked TGF-β2 and induced TGF-β signaling by binding and activating TβRI, leading to the induction of fibrogenic genes. This pathway was enhanced in the presence of an inflammatory cytokine, tumor necrosis factor (TNF)-α, as TNF-α increased the expression of TβRI. Furthermore, we found that NS3 colocalized with TβRI on the surface of an HCV-infected hepatoma cell line, and we observed direct binding between recombinant NS3 and TβRI. These phenomena were reproduced in chimeric mice transplanted with human hepatocytes that had been infected with HCV. These data suggest a novel mechanism by which HCV induces liver fibrosis.

Results

HCV NS3 protease exerted TGF-β mimetic activity via TβRI. To confirm whether HCV NS3 protease might induce the activation of latent TGF-β2, bacterially expressed recombinant NS3 (Supplementary Fig. S1) was incubated with conditioned medium obtained from HEK293T cells transiently overexpressing latent TGF-β2, and the concentration of active TGF-β2 in the reaction mixtures were measured by ELISA. Although the addition of NS3 increased active TGF-β2 concentrations in a dose-dependent manner, these increases were not time-dependent (Supplementary Fig. S2). Instead, we found that NS3 protease itself reacted with TGF-β2 in a dose-dependent manner, as determined by ELISA (Fig. 1A). Next, to assess whether NS3 could induce the bioactivity of TGF-β via TβRI, and whether its activity was dependent on protease activity, we performed a luciferase reporter assay with the TGF-β-responsive $(CAGA)_9$-Luc reporter in CCL64 cells. NS3 demonstrated TGF-β mimetic activity, which was alleviated in the presence of TβRI kinase inhibitors (SB-431542 and LY-364947) in a dose-dependent manner (Fig. 1B). In contrast, an NS3 protease inhibitor, VX-950 (telaprevir), did not affect luciferase activity (Fig. 1B). An unrelated protein with almost the same molecular weight as NS3, HLA class II histocompatibility antigen, DM α chain (HLA-DMA), as well as a carrier-free, tag-control sample, did not exert TGF-β mimetic activity, thus demonstrating the specificity of NS3 (Supplementary Fig. S3). Additionally, an anti-TGF-β2 antibody that detected NS3 in the TGF-β2 ELISA did not inhibit luciferase activity (Supplementary Fig. S4).

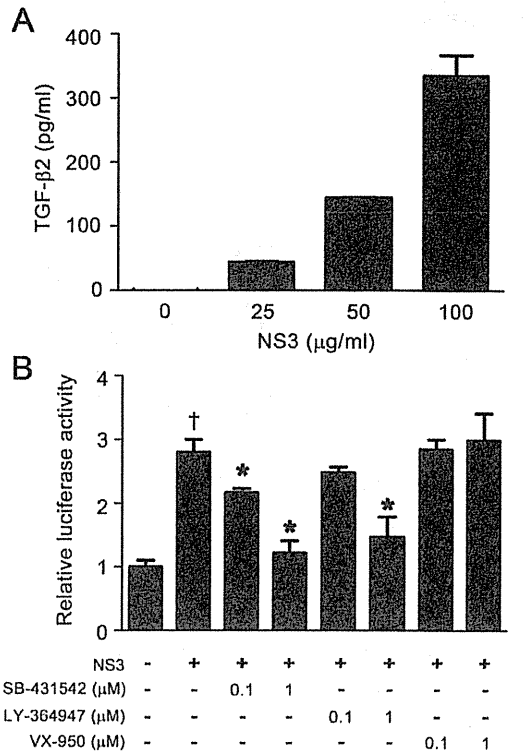

Figure 1 | HCV NS3 protease exerted TGF-β mimetic activity via the type I receptor. (A) TGF-β2 antigenicity of NS3. The indicated concentrations of recombinant NS3 protease were used in the TGF-β2 ELISA assays. (B) TGF-β mimetic activity of NS3 and its suppression by TβRI kinase inhibitors. $(CAGA)_9$-Luc CCL64 cells were stimulated with 100 μg/ml of recombinant NS3 protease for 24 hours, with or without the indicated concentration of TβRI kinase inhibitor or the NS3 protease inhibitor VX-950 (telaprevir). After 24 hours, the cells were harvested and luciferase activity measured. †$p < 0.05$ compared with untreated control cells, *$p < 0.05$ compared with NS3-treated cells without any inhibitors. The data are shown as the mean ± SD (n = 3), and representative results from three independent experiments with similar results are shown.

NS3 stimulated collagen production in hepatic cells, which was augmented by TNF-α. We examined the effect of NS3 on the expression of TGF-β1 and collagen α1 (I) in the human hepatic stellate cell line LX-2. Treatment with NS3 for 12 hours significantly increased both TGF-β1 (1.6-fold) and collagen α1 (I) (1.4-fold) expression in these cells (Fig. 2A). On the contrary, NS3 did not affect the expression of these genes in the normal hepatic cell line Hc. The pretreatment of the cells with tumor necrosis factor-α (TNF-α) enhanced increased TGF-β1 and collagen α1 (I) expression mediated by NS3 and was also accompanied by an increase in TGF-β receptor expression (Fig. 2B). Further increases in TβRI expression were not observed by combination treatment with TNF-α, suggesting that TNF-α increased TβRI expression, which may have enhanced the TGF-β mimetic activity of NS3 in these cells. Furthermore, Smad3 phosphorylation was also induced by NS3 in Hc cells that had been pretreated with TNF-α (Fig. 2D). A similar cooperativity between TNF-α and NS3 protease was not observed in LX-2 cells (Fig. 2C).

Interaction between NS3 and TβRI on the surface of HCV-infected HCC cells. NS3 was immunostained on the surface of HCV-infected Huh-7.5.1 cells both with and without permeabilization. In contrast, an ER marker, calnexin, was only positive after the permeabilization of the cells (Fig. 3A). To examine whether NS3 that was localized to the surface of HCV-infected Huh-7.5.1 cells interacted with TβRI, we performed co-immunostaining (Fig. 3B) and in situ proximity ligation assay (PLA) (Fig. 3C) using antibodies against NS3 and TβRI. Both results showed that NS3 was colocalized and formed a complex with TβRI on the cell surface. Because LX-2 cells (hepatic stellate cells) are not infected with HCV, the data were not recorded. We also co-cultured Huh-7.5.1 infected with HCV and LX-2 cells and examined them using *in situ* PLA. However, the interaction between NS3 protease and TβRI was not observed on the surface of LX-2 cells. Furthermore, we performed co-immunoprecipitation assays using recombinant NS3 and the extracellular domain of TβRI and TβRII. As shown in Figure 3D, FLAG-tagged NS3 bound to TβRI and TβRII, whereas FLAG-tag alone failed to interact with TGF-β receptors (Fig. 3D and Supplementary Fig. S5).

Docking simulation using the Katchalski-Katzir algorithm predicted that NS3 interacts with TβRI at three sites, T22-S42, T76-P96, and G120-S139, in NS3 and F55-M70, I72-V85, and C86-Y99 in TβRI, respectively (Fig. 3E, Table 1, and Supplementary Fig. S6). The predicted binding site peptides, particularly the peptide derived from site 3, completely blocked the interaction between NS3 and

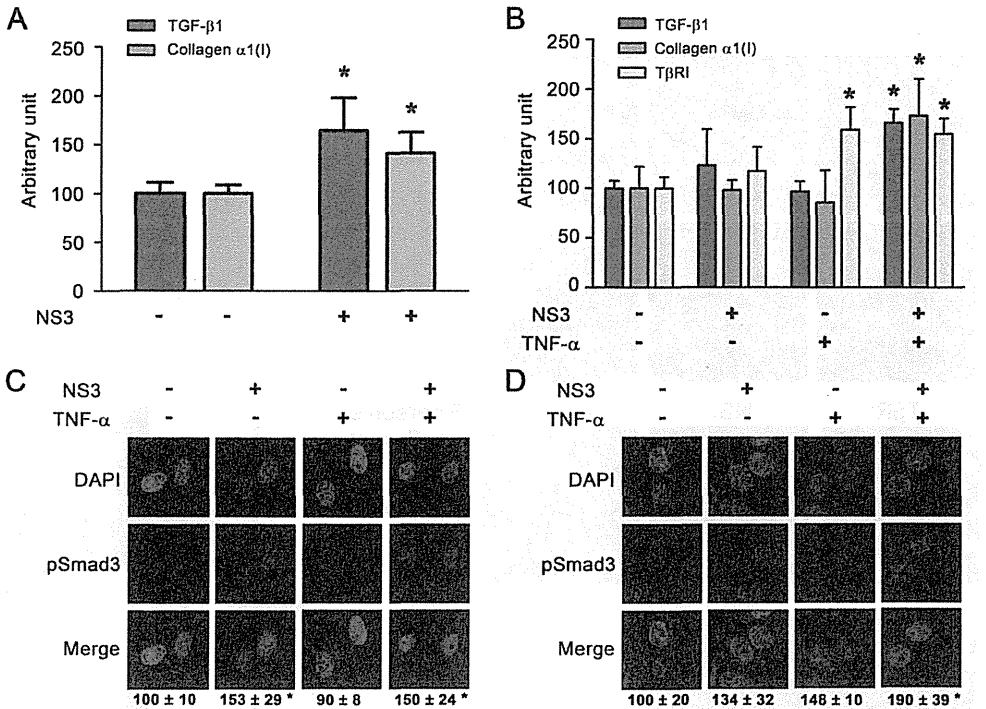

Figure 2 | Cooperativity between NS3 and TNF-α in the stimulation of TGF-β1, collagen α1(I), and TβRI expression. (A) Effect on TGF-β1 and collagen α1(I) mRNA expression in LX-2 cells. The cells were stimulated with 50 μg/ml of NS3 for 12 hours. Total cellular RNA was isolated and reverse transcribed to cDNA, and real-time PCR was performed as described in the Methods section. $*p < 0.05$ compared with untreated control cells. (B) Effect of pretreatment with TNF-α on the stimulation of expression of TGF-β1, collagen α1(I), and TβRI by NS3 protease in HC cells. Following the pretreatment of the cells with 20 ng/ml TNF-α for 12 hours, they were stimulated with 25 μg/ml NS3 for 12 hours, and mRNA expression was measured as described above. $*p < 0.05$ compared with untreated cells. The data are shown as the mean ± SD (n = 3). (C and D) The effect of pretreatment with TNF-α on the stimulation of phosphorylation of Smad3 by NS3 protease in LX-2 cells (C) and Hc cells (D). After the cells were treated with 20 ng/ml TNF-α for 12 hours and 25 μg/ml NS3 for another 12 hours, they were fixed, and immunofluorescent staining was performed as described in the Methods section. The experiments were performed in duplicate. The relative fluorescence intensities of phospho-Smad3 (% of untreated control cells) in 4 randomly selected fields from each dish were calculated with ZEN software and are shown as the mean ± SD. The results are representative of three independent experiments with similar results.

TβRI in the immunoprecipitation experiment (Supplementary Fig. S7A). Antibodies produced to these predicted binding sites within both NS3 and TβRI decreased the TGF-β mimetic activity of NS3 in $(CAGA)_9$-Luc CCL64 cells (Fig. 3F–H). Furthermore, the anti-NS3 antibody inhibited HCV-induced Smad3 phosphorylation (Supplementary Fig. S7B).

Anti-NS3 antibody prevented liver fibrosis in HCV-infected chimeric mice. To test our hypothesis that NS3 exerts TGF-β mimetic activity, thereby causing liver fibrosis, we examined whether the anti-NS3 antibody could prevent liver fibrosis in HCV-infected human hepatocyte-transplanted chimeric mice. The anti-NS3 antibody significantly prevented hepatic collagen accumulation in the mice (Fig. 4A) and decreased the mRNA expression of both TGF-β1 and collagen α1 (I) (Fig. 4B and 4C). There was no significant change in the serum levels of human albumin and HCV RNA during treatment with the anti-NS3 antibody (Supplementary Fig. S8A and S8B).

Discussion

Several groups have studied the molecular mechanisms by which HCV induces liver fibrosis and have reported the following: (i) HCV core protein activates the TGF-β1 promoter via the MAPK pathway in core protein-expressing human hepatocellular carcinoma HepG2 cells[11]; (ii) recombinant core protein upregulates the expression of fibrogenic genes in the human hepatic stellate cell line LX-2 via the toll-like receptor 2 [12] and the obese receptor[13]; and (iii) NS3 protease induces TGF-β1 production in NS3-overexpressing human hepatoma Huh-7 cells[14]. Our data show that NS3 protease mimics TGF-β2 and directly exerts its activity, at least in part, via binding to and activating TβRI, thereby enhancing liver fibrosis. The following experiments should be carried out in the future: effect of NS3 on TβRI phosphorylation, the expression of TGF-β2, TGF-β3, and other TGF-β responsive genes, such as plasminogen activator inhibitor-1, a tissue inhibitor of metalloproteinase-1, and α-smooth muscle actin, to further validate the TGF-β mimetic activity of NS3.

HCV NS3 is a chimera of a helicase and serine protease, which cleaves not only the junction between NS3-4A, NS4A-4B, NS4B-5A, and NS5A-5B for viral polyprotein processing, which is essential to the viral lifecycle, but also the toll-interleukin-1 receptor domain-containing, adaptor-inducing beta interferon, and mitochondrial antiviral signaling protein, which results in the disruption of innate immune responses[7,15]. An NS3 protease inhibitor, telaprevir, which was approved by the FDA in 2011, has been used in triple combination therapy with the current standard treatment of PEGylated interferon and ribavirin[16]. Telaprevir did not inhibit TGF-β mimetic activity in a $(CAGA)_9$-Luc reporter gene assay (Fig. 1C), suggesting that the TGF-β mimetic activity of NS3 is independent of its protease activity.

Much interest has centered on the fact that extraordinarily high concentrations of NS3 protease, up to 100 μg/ml, could exist in

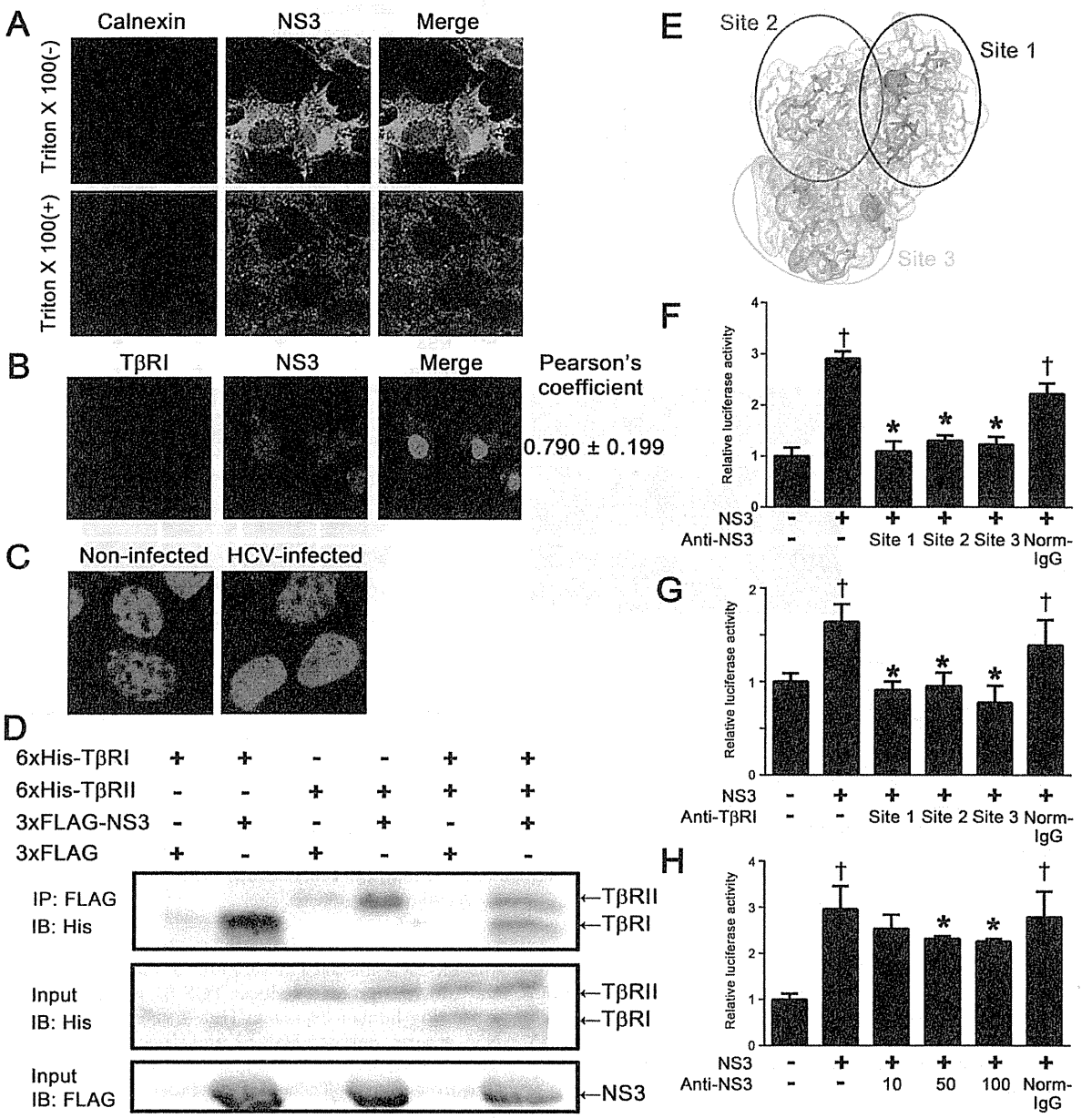

Figure 3 | NS3 protease colocalized and directly interacted with TβRI on the surface of HCV-infected cells. (A) The detection of NS3 protease on the surface of HCV-infected Huh-7.5.1 cells. The cells were fixed, followed ± by permeabilization with Triton-X 100, and then stained with DAPI, anti-NS3 antibody, and anti-calnexin antibody. (B) The colocalization of NS3 protease with TβRI in HCV-infected Huh7.5.1 cells. The cells were fixed and stained with DAPI, anti-NS3 antibody, and anti-TβRI antibody, as described in the Methods section. Pearson's colocalization coefficient values were obtained from 4 randomly selected fields using the ZEN software. The results are shown as the mean ± SD and are representative of three independent experiments with similar results. (C) The detection of NS3-TβRI proximity by in situ PLA in HCV-infected Huh-7.5.1 cells. The red dots indicate interactions between NS3 protease and TβRI, and the nuclei were identified by DAPI staining. (D) The physical interaction of NS3protease with TβRI and TβRII. FLAG-tagged NS3protease was incubated with 6xHis-tagged TβRI and/or TβRII and immunoprecipitated. The coprecipitated proteins were visualized by immunoblotting using anti-His antibody. The gels were run under the same experimental conditions. Cropped blots are shown (full-length blots are presented in Supplementary Fig. S5). (E) The structural overview of the NS3protease. The indicated colored amino acids (site 1, red; site 2, magenta; and site 3, cyan) show the important residues within the putative binding sites to TβRI, and the sequences are presented in Table 1. TGF-β mimetic activity of NS3 was inhibited in the presence of either anti-NS3 polyclonal antibodies against the predicted binding sites of TβRI (F), or anti-TβRI polyclonal antibodies against predicted binding sites of NS3 (G), and anti-NS3 monoclonal antibody against predicted binding site 3 of TβRI (H). Luciferase activities in $(CAGA)_9$-Luc CCL64 cells were measured as before. Normal mouse IgG (Norm-IgG) was used as a negative control. The data are shown as the mean ± SD. †$p < 0.05$ compared with untreated control cells, *$p < 0.05$ compared with NS3-treated cells without any antibodies. Representative results from three independent experiments with similar results are shown.

Table 1 | The amino acid sequences of predicted binding sites between NS3 protease and TβRI

	NS3 protease	TβRI
Site 1	TGRDKNQVEGEVQVVSTATQS	FVSVTETTDKVIHNSM
Site 2	TNVDQDLVGWPAPPGARSLTP	IAEIDLIPRDRPFV
Site 3	GDNRGSLLSPRPVSYLKGSS	CAPSSKTGSVTTTY

The underlined letters denote the putative contact residues.

proximity to a TGF-β receptor. This line of inquiry led us to identify the cooperativity between NS3 and TNF-α, although the cooperative effect was maximal at one fourth this concentration of NS3. Serum levels of TNF-α in chronic hepatitis C patients are known to be significantly higher than those in healthy subjects[17,18]. We showed that TNF-α increased the susceptibility of cells to NS3 by enhancing the expression of TβRI, thereby further increasing the levels of pro-fibrogenic genes (Fig. 2B). Various hepatic cell lines expressed different levels of TβRI, and there appeared to be a threshold in the level of TβRI that enabled cells to produce collagen mRNA upon stimulation with NS3. In particular, Hc cells expressed levels of TβRI below this predicted threshold (Supplementary Fig. S9). Consistent with our findings, carbon tetrachloride has recently been reported to induce acute liver injury, specifically significant liver fibrosis with inflammation, in transgenic mice expressing the full-length HCV polyprotein[19].

We documented the colocalization of NS3 and TβRI on the cell surface of HCV JFH-1-infected Huh-7.5.1 cells (Fig. 3). The results of co-immunoprecipitation and in situ PLA studies supported this conclusion. In future studies, we intend to use mutagenesis experiments of the predicted binding site and competition assays using NS3 and TGF-β in $(CAGA)_9$-Luc CCL64 cells to determine the mechanism of NS3 and TβRI binding. However, at present, how NS3 is released to the extracellular milieu remains to be elucidated. One possibility is that NS3 leaks passively from injured hepatocytes, as is the case for alanine aminotransferase and aspartate aminotransferase. Another possibility is that NS3 is secreted from HCV-infected cells via the Golgi complex. A recent report showed that nonstructural protein (NS) 1 of the dengue virus (DENV) and West Nile virus (WNV) is secreted from DENV- and WNV-infected cells through the Golgi complex following expression in association with the endoplasmic reticulum. Like HCV, these viruses are also members of the family *Flaviviridae*[20].

Zhang et al.[21] identified antibodies against NS3 in the serum of chronic hepatitis C patients and suggested that extracellular NS3 may be present in such cases. However, it remains unclear whether the concentration of HCV NS3 is as high as in our in vitro experiments. Although DENV NS1 has been reportedly detected at high levels (up to 50 μg/ml) in the serum of DENV-infected patients[22], further study is warranted to determine the serum or tissue NS3 concentrations in patients with chronic hepatitis C.

In this study, we generated polyclonal and monoclonal anti-NS3 antibodies that block the NS3-TβRI interaction. All anti-NS3 and anti-TβRI polyclonal antibodies generated against the predicted binding sites almost completely blocked TGF-β mimetic activity. This finding was likely due to steric hindrance by these antibodies or a requirement of binding at all three sites for signal transduction by NS3. The monoclonal antibody is a powerful tool that can be used to explore our working hypothesis that NS3 enhances liver fibrosis via the TGF-β receptor *in vivo*. We showed that the anti-NS3 monoclonal antibody generated against a predicted binding site to TβRI ameliorated liver fibrosis in HCV-infected human hepatocyte transplanted chimeric mice (Fig. 4A–C). The control of fibrosis after the eradication of the virus determines the prognosis, including the likelihood of progression to tumorigenesis. Therefore, the NS3 antibody

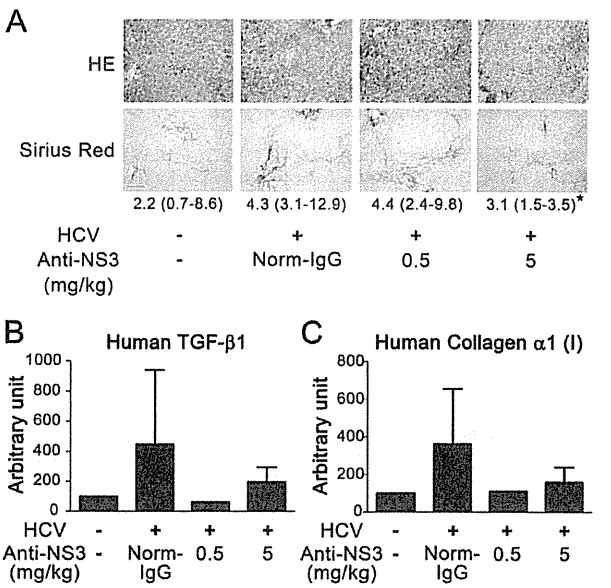

Figure 4 | Anti-NS3 antibody attenuated liver fibrosis in the HCV-infected chimeric mice. (A) Staining of liver sections. Paraffin sections were prepared from the livers of HCV-infected chimeric mice 16 weeks after HCV inoculation, and stained with hematoxylin and eosin (upper panels) and Sirius Red (lower panels). An anti-NS3 antibody was administered at the indicated doses, and normal mouse IgG (Norm-IgG) was administered at a dose of 5 mg/kg. For each group, the median ratios in Sirius Red positive/total area (%) from 6 randomly selected fields are shown, with the range in parentheses. $*p < 0.05$ compared with HCV-infected mice without anti-NS3 antibody. Scale bar = 100 μm. The representative result from 6 randomly selected fields is shown. (B) and (C) Hepatic mRNA expression in HCV-infected chimeric mice. Total RNA was isolated from the livers of these mice and reverse transcribed to cDNA, and real-time PCR was performed as described in the Methods section to quantitate the expression of human TGF-β1 expression (B) and human collagen α1 (I) (C). The data are shown as the mean ± SD, and representative results from two independent experiments with similar results are shown.

against the TβRI binding site might have a clinical benefit in HCV patients with cirrhosis after combination therapy.

In conclusion, we demonstrated for the first time that HCV NS3 protease serves as a novel TGF-β receptor ligand and enhances liver fibrosis. This phenomenon might be beneficial to the virus, as TGF-β signals suppress host immunity. Our results provide elucidation regarding the molecular mechanism by which HCV induces liver fibrosis.

Methods

Materials. SB-431542 and LY-364947 were purchased from Sigma-Aldrich (St. Louis, MO). Recombinant human TNF-α was purchased from R&D systems, Inc. (Minneapolis, MN). Anti-NS3 antibody and anti-calnexin antibody were purchased from Abcam (Cambridge, UK). Anti-TβRI antibody and anti-phospho-Smad3 antibody were purchased from Santa Cruz Biotechnology (Santa Cruz, CA) and Immuno-Biological Laboratories (Gunma, Japan), respectively. Anti-Flag M2 antibody and anti-His antibody were purchased from Sigma (St. Louis, MO). Anti-NS3 antibodies and anti-TβRI antibodies against predicted binding sites were provided by the BioMatrix Research Institute (Chiba, Japan).

Cell culture. $(CAGA)_9$-Luc CCL64 cells were kindly provided by Prof. Hideaki Kakeya (Kyoto University, Kyoto, Japan), the hepatic stellate cell line LX-2 was kindly provided by Prof. Norifumi Kawada (Osaka City University, Osaka, Japan), and the human hepatoma cell line Huh-7.5.1 were maintained in Dulbecco's modified Eagle's medium (DMEM) supplemented with 10% fetal bovine serum, penicillin, and streptomycin. HC cells, a normal human hepatocyte cell line purchased from Cell Systems (Kirkland, WA), were cultured in CS-C complete medium (Kirkland, WA).

Protein preparation. The N-terminal histidine or 3xFLAG-tagged NS3 protease, and the extracellular domain of human TβRI and TβRII were expressed in *Escherichia coli* by isopropyl-β-thiogalactopyranoside induction. The protein was purified by affinity chromatography in a HisTrap HP column (GE Healthcare, Waukesha, WI). Detailed procedures are in the Supplementary information.

Enzyme-linked immunosorbent assay (ELISA). TGF-β2 ELISA was performed using a TGF-β2 Emax® Immune Assay System ELISA kit (Promega, Madison, WI) according to the manufacturer's instructions.

Luciferase assay. The mink lung epithelial cell line CCL64, which stably expressed $(CAGA)_9$-MLP-luciferase and contained nine copies of a Smad-binding CAGA box element upstream of a minimal adenovirus major late promoter (2×10^4 cells/well)[23], was seeded into 96-well plates. The next day, the medium was replaced with fresh medium containing 0.1% bovine serum albumin, and the cells were cultured for an additional 24 hours. The cells were extracted with lysis buffer, and luciferase activity was measured by a Luciferase Assay System (Promega, Madison, WI) according to the manufacturer's instructions.

Real-time RT-PCR. The isolation of total RNA and real-time RT-PCR were performed as described previously[24]. Briefly, total RNA was extracted using the RNeasy mini kit (Qiagen, Valencia, CA) according to the manufacturer's protocols. RNA (0.5 μg) was reverse transcribed to cDNA using the PrimeScript® RT Master Mix (Takara Bio Inc., Shiga, Japan). The mRNA expression levels were determined using real-time PCR. Real-time PCR was performed with the Thermal Cycler Dice® Real Time System, using the SsoAdvanced™ SYBR® Green Supermix (Bio-Rad Laboratories, Hercules, CA) and normalized to GAPDH mRNA expression. The primer sequences used were as follows: human TGF-β1 forward: 5′-ACT ATT GCT TCA GCT CCA CGG A-3′, reverse: 5′-GGT CCT TGC GGA AGT CAA TGT A-3′; human collagen α1 (I) forward: 5′-ACG AAG ACA TCC CAC CAA TC-3′, reverse: 5′-AGA TCA CGT CAT CGC ACA AC-3′; human GAPDH forward: 5′-GGA GTC AAC GGA TTT GGT-3′, reverse: 5′-AAG ATG GTG ATG GGA TTT CCA-3′; and human TβRI forward: 5′-CTT AAT TCC TCG AGA TAG GC-3′, reverse: 5′-GTG AGA TGC AGA CGA AGC-3′.

Immunofluorescence staining. The cells were grown on eight-well chamber slides or glass bottom dishes and were incubated with HCV virion for 24 hours at 37°C. The cells were washed with PBS, fixed with 4% paraformaldehyde for 10 min at room temperature, and permeabilized with 0.1% Triton X-100 for 20 min at room temperature. After blocking with 3% BSA/10% normal goat serum/PBS for 30 min, the cells were incubated with primary antibodies for 2 hours, followed by incubation with secondary antibodies for 30 min at RT. For detecting NS3 and TβRI on the cell surface, the cells were fixed without permeabilization after incubation with the secondary antibodies. After being washed with PBS, the cells were mounted with Vectashield DAPI mounting medium (Vector Laboratories, Inc., Burlingame, CA) and observed under a Zeiss LSM 700 laser scanning confocal microscope. For quantitative fluorescence analyses, the intensity of phosphorylated Smad3 and the colocalization of NS3 and TβRI (Pearson's colocalization coefficient values) in each panel were calculated with ZEN software.

Proximity ligation assay (PLA). HCV-infected Huh-7.5.1 cells were fixed with 4% paraformaldehyde for 10 min at room temperature and subjected to in situ PLA using a Duolink in situ red starter kit (Olink Bioscience, Uppsala, Sweden) according to the manufacturer's instructions. Briefly, cells were blocked and incubated with primary antibodies against NS3 and TβRI, followed by incubation with the PLA probes, which were secondary antibodies (anti-mouse and anti-rabbit) conjugated to oligonucleotides. DNA ligase was added to enable the formation of circular DNA strands when the PLA probes were in close proximity. This step was followed by incubation with oligonucleotides and polymerase for rolling circle amplification[25]. Texas red-labeled oligonucleotides, which hybridize to the amplified products, were used for visualization. The cells were observed under a Zeiss LSM 700 laser scanning confocal microscope.

Immunoprecipitation and immunoblotting. Anti-FLAG M2 affinity beads were pretreated with 5% bovine serum albumin in 20 mM Tris-HCl, pH 7.5, 150 mM NaCl overnight. Isotype control IgG was bound to Protein G PLUS-Agarose (Santa Cruz) pretreated with 5% bovine serum albumin in 20 mM Tris-HCl, pH 7.5, 150 mM NaCl. Cell lysates with 3xFLAG or 3x-FLAG-NS3 (2 mg protein) were incubated with 50 μl of the beads (10% slurry) at 4°C for 3 hours. The beads were then washed three times with the lysis buffer and incubated with lysates containing 6xHis-TβRI or 6xHis-TβRII (0.5 mg protein) at 4°C overnight. The bound proteins were eluted with the SDS-PAGE sample buffer after washing four times with the lysis buffer and then were subjected to SDS-PAGE (15% acrylamide) followed by transfer onto a PVDF membrane (Pall). The proteins were then visualized using anti-His tag HRP DirectT (MBL, 1/5000) or anti-FLAG BioM2 antibody (Sigma, 10 μg/ml) and horseradish peroxidase-conjugated anti-biotin antibody (Cell Signaling) using the ECL Western blotting detection reagent (GE Healthcare).

In silico docking simulation. The protein-protein docking simulation was implemented based on the geometric complementarity[26] between NS3 protease (PDB ID, 1NS3) and TβRI (PDB ID, 2PJY). Specifically, coordinates of the proteins were projected onto three-dimensional grids separated from each other at regular intervals. A surface score and an intramolecular score were assigned to each grid. This operation was conducted for both the receptor and the ligand. Next, convolution between the obtained grids was performed, the surfaces were explored exhaustively, and the complementarities of the binding states were calculated based on the scores. Amino acid residues appearing frequently in binding states with high complementarity scores can be estimated to be residues that are highly likely to appear in the interaction with an actual receptor. Accordingly, amino acid residues with an interatomic distance of 3.8 Å or less in the putative binding states were defined as contact residues and regarded as the putative contact residues of NS3 and TβRI.

Animal experiment. Chimeric mice with humanized livers were generated as previously described using urokinase-type plasminogen activator (uPA)-transgenic/SCID mice[27]. All mice were transplanted with frozen human hepatocytes obtained from a single donor. All animal experiments were approved by RIKEN Institutional Animal Use and Care Administrative Advisory Committees and were performed in accordance with RIKEN guidelines and regulations. Infection, extraction of serum samples, and euthanasia were performed under isoflurane anesthesia. Male chimeric mice (12- to 14-week old) were intravenously injected with 100 μl HCV J6/JFH-1 strain (1×10^8 copies/ml). Four weeks after HCV inoculation, anti-NS3 antibodies against predicted binding sites with the TβRI receptor were administered at doses of 0.5 mg/kg of BW or 5 mg/kg of BW twice a week for twelve weeks. Normal mouse IgG was administered at a dose of 5 mg/kg of BW as a control. When the animals were euthanized, the livers were either fixed with 4% paraformaldehyde for histological analysis or frozen immediately in liquid nitrogen for mRNA isolation.

Staining of liver tissue sections. The liver tissues were fixed in 4% paraformaldehyde and embedded in paraffin, and tissue sections (6 μm in thickness) were prepared with a Leica sliding microtome (Leica Microsystems, Nussloch, Germany). The liver tissue sections were deparaffinized, rehydrated, and incubated for 5 min with a drop of Proteinase K (Dako Envision) in 2 mL of 0.05 M Tris-HCl buffer (pH 7.5) at room temperature. The liver tissue sections were stained with Mayer's hematoxylin solution (Muto Chemicals) and 1% eosin Y solution (Muto Chemicals). Sirius Red, which results in a red staining of all fibrillar collagen, was used to evaluate fibrosis. Briefly, the liver sections were stained with 0.05% Fast Green FCF (ChemBlink, Inc. CAS: 2353-45-9) and 0.05% Direct Red 80 (Polysciences, Inc. CAS: 2610-10-18) in saturated picric acid (Muto Chemicals) for 90 min at room temperature. The ratios of Sirius Red positive/total area (%) from 6 randomly selected fields were measured for each group using WinROOF software (Mitani Corp., Tokyo, Japan).

Statistics. Statistical analysis was performed using one-way analysis of variance, followed by Dunnett's post-hoc test. A two-tailed Student's *t*-test was used to evaluate differences between the two groups. The Kruskal-Wallis test followed by Dunn's post-hoc test was used for multiple comparisons of Sirius Red positive areas.

1. Marazzi, I. *et al.* Suppression of the antiviral response by an influenza histone mimic. *Nature* **120**, 428–433 (2012).
2. Chaurushiya, M. S. *et al.* Viral E3 ubiquitin ligase-mediated degradation of a cellular E3: viral mimicry of a cellular phosphorylation mark targets the RNF8 FHA domain. *Mol. Cell.* **123**, 352–364 (2012).
3. Tong, M. J., el-Farra, N. S., Reikes, A. R. & Co, R. L. Clinical outcomes after transfusion-associated hepatitis C. *N. Engl. J. Med.* **332**, 1463–1466 (1995).
4. Poynard, T., Yuen, M. F., Ratziu, V. & Lai, C. L. Viral hepatitis C. *Lancet* **362**, 2095–2100 (2003).
5. Lavanchy, D. Chronic viral hepatitis as a public health issue in the world. *Best Pract Res Clin. Gastroenterol.* **22**, 991–1008 (2008).
6. Moradpour, D., Penin, F. & Rice, C. M. Replication of hepatitis C virus. *Nat. Rev. Microbiol.* **5**, 453–463 (2007).
7. Raney, K. D., Sharma, S. D., Moustafa, I. M. & Cameron, C. E. Hepatitis C virus non-structural protein 3 (HCV NS3): a multifunctional antiviral target. *J. Biol. Chem.* **285**, 22725–22731 (2010).
8. Okuno, M. *et al.* Prevention of rat fibrosis by protease inhibitor, Camostat Mesilate, via reduced generation of active TGF-β. *Gastroenterology* **120**, 1784–1800 (2001).
9. Akita, K. *et al.* Impaired liver regeneration in mice by lipopolysaccharide via TNF-α/kallikrein-mediated activation of latent TGF-β. *Gastroenterology* **123**, 352–364 (2002).
10. Ikushima, H. & Miyazono, K. TGFβ signalling: a complex web in cancer progression. *Nat. Rev. Cancer* **10**, 415–424 (2010).
11. Taniguchi, H. *et al.* Hepatitis C virus core protein upregulates transforming growth factor-β1 transcription. *J. Med. Virol.* **72**, 52–59 (2004).
12. Coenen, M. *et al.* Hepatitis C virus core protein induces fibrogenic actions of hepatic stellate cells via toll-like receptor 2. *Lab. Invest.* **91**, 1375–1382 (2011).
13. Wu, C. F., Lin, Y. L. & Huang, Y. T. Hepatitis C virus core protein stimulates fibrogenesis in hepatic stellate cells involving the obese receptor. *J. Cell. Biochem.* **114**, 541–550 (2012).
14. Presser, L. D., Haskett, A. & Waris, G. Hepatitis C virus-induced furin and thrombospondin-1 activate TGF-β1: Role of TGF-β1 in HCV replication. *Virology* **412**, 286–296 (2011).

15. Romano, K. P. *et al.* Molecular mechanisms of viral and host cell substrate recognition by hepatitis C virus NS3/4A protease. *J. Virol.* **85**, 6106–6116 (2011).
16. Kwong, A. D., Kauffman, R. S., Hurter, P. & Mueller, P. Discovery and development of telaprevir: an NS3-4A protease inhibitor for treating genotype 1 chronic hepatitis C virus. *Nat. Biotechnol.* **29**, 993–1003 (2011).
17. Toyoda, M. *et al.* Role of serum soluble Fas/soluble Fas ligand and TNF-α on response to interferon-α therapy in chronic hepatitis C. *Liver* **20**, 305–311 (2000).
18. Lecube, A., Hernandez, C., Genesca, J. & Simo, R. Proinflammatory cytokines, insulin resistance, and insulin secretion in chronic hepatitis C patients: A case-control study. *Diabetes Care* **29**, 1096–1101 (2006).
19. Chouteau, P. *et al.* Hepatitis C virus (HCV) protein expression enhances hepatic fibrosis in HCV transgenic mice exposed to a fibrogenic agent. *J. Hepatol.* **57**, 499–507 (2012).
20. Muller, D. A. & Young, P. R. The flavivirus NS1 protein: Molecular and structural biology, immunology, role in pathogenesis and application as a diagnostic biomarker. *Antiviral Res.* **98**, 192–208 (2013).
21. Zhang, Z. X., Sonnerborg, A. & Sallberg, M. A cell-binding Arg-Gly-Asp sequence is present in close proximity to the major linear antigenic region of HCV NS3. *Biochem. Biophys. Res. Commun.* **202**, 1352–1356 (1994).
22. Alcon, S. *et al.* Enzyme-linked immunosorbent assay specific to Dengue virus type 1 nonstructural protein NS1 reveals circulation of the antigen in the blood during the acute phase of disease in patients experiencing primary or secondary infections. *J. Clin. Microbiol.* **40**, 376–81 (2002).
23. Datta, P. K. & Moses, H. L. STRAP and Smad7 synergize in the inhibition of transforming growth factor beta signaling. *Mol. Cell. Biol.* **20**, 3157–3167 (2000).
24. Tatsukawa, H. *et al.* Role of transglutaminase 2 in liver injury via cross-linking and silencing of transcription factor Sp1. *Gastroenterology* **136**, 1783–1795 (2009).
25. Soderberg, O. *et al.* Characterizing proteins and their interactions in cells and tissues using the *in situ* proximity ligation assay. *Methods* **45**, 227–232 (2008).
26. Katchalski-Katzir, E. *et al.* Molecular surface recognition: determination of geometric fit between proteins and their ligands by correlation techniques. *Proc. Natl. Acad. Sci. USA* **89**, 2195–2199 (1992).
27. Tateno, C. *et al.* Near completely humanized liver in mice shows human-type metabolic responses to drugs. *Am. J. Pathol.* **165**, 901–912 (2004).

Acknowledgments

We are indebted to Mr. Kazushige Katsura and Ms. Chiemi Mishima-Tsumagari (RIKEN Systems and Structural Biology Center, Kanagawa, Japan; Division of Structural and Synthetic Biology, RIKEN Center for Life Science Technologies, Yokohama, Japan) for preparing and providing recombinant NS3, and Dr. Takashi Shimada, Dr. Chise Tateno, and Dr. Masakazu Kakuni (PhenixBio Co., Ltd., Hiroshima, Japan) for helpful discussions regarding the animal experiment. This work was supported in part by a Grant-in-Aid for Scientific Research from the Ministry of Education, Culture, Sports, Science and Technology (23390202 to S.K.), and Grants for Collaborative Researchers from Industries (to K.S.), Program for Drug Discovery and Medical Technology Platforms (to S.K.), and Chemical Genomics Research Program (to S.K.) from RIKEN.

Author contributions

Sakata K., Hara M. and Yaguchi S. performed experiments. Sakata K., Matsuura T., Miyazawa K., Imoto M. and Kojima S. wrote the manuscript. Terada T., Matsumoto T., Shirouzu M., Yokoyama S., Yamaguchi T. and Suzuki T. contributed to the production and the purification of recombinant NS3 and its antibodies. Watanabe N., Aizaki H. and Wakita T. contributed to the production and the purification of HCV and discussion from the point of view of virology. Takaya D. performed docking simulation to predict binding sites. Sakata K. and Kojima S. planned the research. Kojima S. supervised the entire project.

Additional information

Supplementary information accompanies this paper at http://www.nature.com/scientificreports

Competing financial interests: The authors declare no competing financial interests.

How to cite this article: Sakata, K. *et al.* HCV NS3 protease enhances liver fibrosis via binding to and activating TGF-β type I receptor. *Sci. Rep.* **3**, 3243; DOI:10.1038/srep03243 (2013).

ELSEVIER

Institut Pasteur

Microbes and Infection 15 (2013) 45–55

www.elsevier.com/locate/micinf

Original article

Selective estrogen receptor modulators inhibit hepatitis C virus infection at multiple steps of the virus life cycle

Yuko Murakami [a,*], Masayoshi Fukasawa [b], Yukihiro Kaneko [a], Tetsuro Suzuki [c,1], Takaji Wakita [c], Hidesuke Fukazawa [a]

[a] *Department of Bioactive Molecules, National Institute of Infectious Diseases, Toyama 1-23-1, Shinjuku-ku, Tokyo 162-8640, Japan*
[b] *Department of Biochemistry and Cell Biology, National Institute of Infectious Diseases, Tokyo, Japan*
[c] *Department of Virology II, National Institute of Infectious Diseases, Tokyo, Japan*

Received 15 June 2012; accepted 13 October 2012
Available online 23 October 2012

Abstract

We screened for hepatitis C virus (HCV) inhibitors using the JFH-1 viral culture system and found that selective estrogen receptor modulators (SERMs), such as tamoxifen, clomifene, raloxifene, and other estrogen receptor α (ERα) antagonists, inhibited HCV infection. Treatment with SERMs for the first 2 h and treatment 2–24 h after viral inoculation reduced the production of HCV RNA. Treating persistently JFH-1 infected cells with SERMs resulted in a preferential inhibition of extracellular HCV RNA compared to intracellular HCV RNA. When we treated two subgenomic replicon cells, which harbor HCV genome genotype 2a (JFH-1) or genotype 1b, SERMs reduced HCV genome copies and viral protein NS5A. SERMs inhibited the entry of HCV pseudo-particle (HCVpp) genotypes 1a, 1b, 2a, 2b and 4 but did not inhibit vesicular stomatitis virus (VSV) entry. Further experiment using HCVpp indicated that tamoxifen affected both viral binding to cell and post-binding events including endocytosis. Taken together, SERMs seemed to target multiple steps of HCV viral life cycle: attachment, entry, replication, and post replication events. SERMs may be potential candidates for the treatment of HCV infection.

Keywords: HCV; Tamoxifen; SERM (Selective estrogen receptor modulator)

1. Introduction

Over 170 million people in the world are infected with the hepatitis C virus (HCV). Approximately 20% of infected patients develop cirrhosis and hepatocellular carcinoma after chronic HCV infection. No HCV vaccine is available yet, and the current standard of care, which consists of a combination of interferon (IFN) and ribavirin, is only effective for approximately 50% of infected patients, and many patients have serious side effects. Because of the urgent need for novel HCV therapeutics, research is being conducted to develop new anti-HCV drugs. In addition to *in vitro* screening assays that target HCV-specific enzymes, other approaches that use replicon cells and the recently described Huh 7.5.1-JFH-1 (genotype 2a)-infection system have been developed [1]. The Huh 7.5.1-JFH-1-infection system is an excellent system to identify HCV inhibitors that interfere with individual steps of the HCV life cycle, such as viral attachment, entry, and release. This experimental system allows both viral and host components that are involved in HCV infection to be targeted. Although drugs that target the host components may be toxic, such drugs are unlikely to select for resistant viruses.

We screened chemicals using a cell-based screening system [2] and found that tamoxifen and other selective estrogen receptor modulators (SERMs) inhibited HCV infection. Tamoxifen has been successfully used for the treatment of breast cancer since it was found to be an ER antagonist over 30 years ago. Clomifene and raloxifene, which are compounds

* Corresponding author. Tel.: +81 3 5285 1111x2327; fax: +81 3 5285 1272.
E-mail address: murakami@nih.go.jp (Y. Murakami).
[1] Present address: Department of Infectious Diseases, Hamamatsu University School of Medicine, Hamamatsu, Japan.

1286-4579/$ - see front matter © 2012 Institut Pasteur. Published by Elsevier Masson SAS. All rights reserved.
http://dx.doi.org/10.1016/j.micinf.2012.10.003

that are related to tamoxifen, have been developed and used for the treatment of breast cancer and for the treatment of anovulation and osteoporosis. Currently, these three SERMs and toremifene have been approved in Japan and the US, and next-generation SERMs are undergoing clinical evaluation.

Because tamoxifen exhibited the ability to inhibit HCV infection, we determined which SERMs could effectively inhibit HCV infection and be approved for clinical use. The first-generation SERMs—tamoxifen, clomifene, and raloxifene—were all effective against HCV as were other ERα antagonists. We examined whether SERMs could be utilized as new drugs for the treatment of HCV.

2. Materials and methods

2.1. Cells and virus

Human hepatoma cell line, Huh 7.5.1 cells and human embryonic kidney 293T cells were cultured in Dulbecco's modified Eagle's medium (DMEM) (Sigma–Aldrich Co. St. Louis, MO, USA) with 10% fetal bovine serum (FBS). HCV-JFH-1 (HCVcc) (genotype 2a) was the culture supernatant of infected Huh 7.5.1 cells as described previously [2]. A subgenomic replicon cell line, clone #4-1, which harbors the genotype 2a (JFH-1) [3,4], and clone #5-15, that harbors the genotype 1b HCV genome [5], were also cultured in DMEM with FBS.

2.2. Chemicals

The SCADS inhibitor kit I was provided by the Screening Committee of Anticancer Drugs, supported by a Grant-in-Aid for Scientific Research on the Priority Area "Cancer" from The Ministry of Education, Culture, Sports, Science and Technology of Japan. Tamoxifen, diethylstilbestrol, triphenylethylene, 17β-estradiol, and brefeldin A were purchased from Sigma–Aldrich Co. (St. Louis, MO, USA). Clomifene was purchased from LKT Laboratories, Inc. (St. Paul, MN, USA), and hydroxytamoxifen ((z)-4-hydroxytamoxifen) and raloxifene were purchased from Enzo Life Sciences, Inc. (Farmingdale, NY, USA). Chloroquine was purchased from WAKO (Osaka, Japan). Other chemicals were purchased from Tocris Bioscience (Bristol, UK).

2.3. Quantification of the viral titer in medium

Huh 7.5.1 cells were seeded in 96-well plates at a density of 2×10^4 cells per well in a volume of 120 μl. The next day, 15 μl of media that contained the test compound and 15 μl of the HCVcc virus stock solution at a moi of 0.01 were added to each well. After 5 days, 100 μl of the culture supernatant was taken from each well, and viral RNA was extracted. Total RNA was also extracted from the cells. Quantitative real-time RT-PCR was then performed with One step SYBR PrimeScript RT-PCR Kit (Takara-Bio Co., Otsu, Japan) as described previously [2]. In the case of #4-1 replicon cell, as an internal control, glyceraldehyde-3-phosphate dehydrogenase (GAPDH) were measured with primers 5′-CCACCCATGGCAAATTCC-3′ and 5′-TGGGATTTCCATTGAT-3′. Cell growth was monitored using the MTT assay as described previously [6].

2.4. Western blotting

Western blotting was performed as previously described [2]. Briefly, cell lysates that contained equal quantities of protein were separated by SDS-PAGE, transferred onto PVDF membranes, and probed with antibodies against the core antigen (2H9), NS5A (Austral Biologicals, San Raman, CA, USA), or GAPDH (Santa Cruz Biotech. Inc., Santa Cruz, USA). After incubation with horseradish peroxidase-conjugated secondary antibodies, the protein bands on the PVDF membranes were detected using an ECL system (GE Healthcare UK Ltd., Amersham Place, UK).

2.5. Production of and infection with pseudo-particles

HCV pseudo-particles (HCVpp) were generated using the following 3 plasmids: a Gag-Pol packaging construct (Gag-Pol 5349), a transfer vector construct (Luc 126), and a glycoprotein-expressing construct (HCV E1E2) (JFH-1, 2a). The generation of the pseudo-particles was performed according to the method described by Bartosch et al. [7]. To express the glycoproteins of other HCV genotypes, HCV E1E2 constructs of the genotypes 1a (H77), 1b (UKN1B 12.6), 2b (UKN2B 2.8), and 4 (UKN4 11.1) were generously provided by Dr. F. Cosset (INSERM, France) [8]. To produce VSVpp, a plasmid that coded the vesicular stomatitis virus (VSV) envelope, pCAG-VSV, was generously provided by Dr. Y. Matsuura (Osaka University, Japan). Gag-Pol 5349 (3.1 μg), Luc 126 (3.1 μg), and each of the individual glycoprotein-expression constructs (1.0 μg) were co-transfected into 293T cells that were seeded on a 10-cm dish (2.5×10^6 cells) using TransIT-LT1 Transfection Reagent (21.6 μl) (Mirus Bio LLC, Madison, WI, USA). The medium from the transfected cell cultures was harvested and used as the pseudo-particle stock. For the infection assay, Huh 7.5.1 cells were seeded onto a 48-well plate at a density of 4×10^4 cells per well one day prior to infection. The medium was then removed, and the cells were subsequently infected with the pseudo-particles in the presence or absence of drug. The cells were then incubated for 3 h. The VSVpp preparation was diluted (1:600) to infect with similar RLU activity compared to the HCVpp. The supernatant was then removed, fresh culture medium was added to the cells, and the cells were incubated for an additional 3 days. The luciferase assays were performed using a luciferase assay system (Promega Co. Madison WI, USA). Anti-CD81 antibody (sc-23962) was purchased from Santa Cruz Biotech.

3. Results

3.1. Tamoxifen and estrogen receptor α antagonists inhibited HCV infection

Using quantitative RT-PCR, we screened the compounds in the SCADS inhibitor kit I. Drugs and HCVcc at a moi of 0.01

were added to Huh 7.5.1 cells. Five days later, the quantity of HCV RNA in the culture supernatant was measured using quantitative real-time RT-PCR [2]. We found that tamoxifen reduced the levels of JFH-1 RNA in the culture supernatant. We also examined the effects of other SERMs and agonists and antagonists of ERα. As shown in Fig. 1, tamoxifen, clomifene, and hydroxytamoxifen, which have a triphenylethylene backbone, exhibited intense inhibitory effects (EC_{50}: approximately 0.1 μM). Triphenylethylene showed reduced inhibitory activity (data not shown). Raloxifene also inhibited viral RNA production at a similar concentration. (EC_{50}: approximately 0.1 μM) (Fig. 1a). Tamoxifen and raloxifene display both ERα antagonist and agonist properties in a dose- and tissue-dependent manner [9]. In contrast, ICI 182,780 (fulvestrant), ZK164015, and MPP (methyl-piperidino-pyrazole) are exclusively antagonistic [10–12]. These ERα antagonists also showed inhibitory activity against JFH-1, but their EC_{50} values were approximately 1 μM (Fig. 1b). As the 50% toxic concentrations (TC_{50}) for these compounds were observed to be greater than 10 μM (Fig. 1a and b), these specific indexes are over 100. In contrast, the ERα agonists 17β-estradiol, diethylstilbestrol, and PPT (1,3,5-tris(4-hydroxyphenyl)-4-propyl-1*H*-pyrozole) did not inhibit HCV (Fig. 1c). As expected, the SERMs that were observed to effectively inhibit HCV RNA production also reduced the core protein levels intracellularly (Fig. 1d).

3.2. SERMs inhibited more than one step of the JFH-1 life cycle

To determine which step of the JFH-1 life cycle was inhibited by the SERMs studied, we performed time-of-addition experiments. As described previously [2], JFH-1 appears to complete one infectious life cycle in approximately 48 h. Huh 7.5.1 cells were inoculated with JFH-1-containing medium (moi 0.1) with or without drug and were then incubated for 2 h. After the medium was removed, fresh medium with or without drug was added. The cells were then incubated for another 46 h. Treatment with 10 μM tamoxifen for 48 h reduced the amount of viral RNA in the medium to 1.7% of levels observed in the control. Treatment with tamoxifen for the first 2 h after infection (0–2 h) reduced viral RNA to 2.3% of the levels observed in the control. The addition of tamoxifen to the fresh medium just after the removal of the virus (2–48 h) resulted in a reduction in the amount of viral RNA to 10.7% of the levels observed in the control. The addition of tamoxifen 24 h after viral inoculation (24–48 h) resulted in a decrease in the amount of viral RNA to 60% of the levels observed in the control (Fig. 2a). This result suggests that tamoxifen inhibits mainly viral entry and some steps during replication. 10 μM of raloxifene exhibited a similar inhibitory pattern but less inhibited by the treatment after the entry step (Fig. 2b). A pure ERα antagonist, ICI 182,780 (30 μM), also exhibited inhibition of both viral entry and the replication steps, but the inhibition of the entry step was not so marked (Fig. 2c).

To further investigate effect on HCV post replication, we infected HCV in the presence of the drugs for 72 h (moi 0.1) and examined their effects on intracellular and extracellular HCV RNA levels. Brefeldin A, an inhibitor of protein transport [13], was used as a positive control of post replication inhibition. In this experimental setting, brefeldin A showed intracellular HCV RNA accumulation suggesting post replication inhibition (Fig. 2d). SERMs generally reduced HCV RNA in cell as well as HCV RNA in medium, although the extent of reduction was different (Fig. 2d). Lower concentration of SERMs reduced extracellular HCV RNA more robustly than intracellular HCV RNA. At a concentration of 0.1 μM, tamoxifen exclusively inhibited HCV RNA in the culture supernatant but not intracellular HCV RNA levels, in a manner similar to that of brefeldin A (Fig. 2d). The results suggest that SERMs inhibit post replication step(s) such as assembly or release. Because low concentrations of tamoxifen failed to inhibit intracellular HCV RNA, SERMs potentially target post replication step(s) more efficiently than replication step. In this condition, higher concentrations (1 and 3 μM) of tamoxifen seemed to inhibit intracellular HCV RNA rather than extracellular HCV RNA, although the reason is not clear.

To determine the effect of these drugs on chronic infection, we used pre-infected Huh 7.5.1 cells. We infected the cell with HCVcc at a moi of 0.01 and incubated for 3 days. Three days after infection, the drugs were added, and the cells were further incubated for 48 h. At the time of drug addition, the cells were persistently infected, and HCVcc was continuously produced and released into the culture supernatant, which is similar condition to chronic infection. HCV RNA was extracted from the culture supernatant and the cells after 48 h and measured copy number of HCV RNA. Both HCV RNA in the culture supernatant and that in the cell were reduced by treatment with the SERMs, but the intracellular HCV RNA levels were less reduced (Fig. 2e). This suggested that the SERMs caused preferential reduction in extracellular HCV RNA through interference with some post replication step(s), such as assembly or release. Brefeldin A accumulated intracellular HCV RNA, and reduced HCV RNA level in the culture supernatant (Fig. 2e).

These data suggested that the SERMs inhibit multiple steps in the HCV life cycle: entry, viral RNA replication and some post replication step(s).

3.3. SERMs inhibited copies and NS5A protein expression in replicon cells

To confirm the effect of these drugs on viral replication, we used two subgenomic replicon cells. The subgenomic replicon cells, derived from Huh7 cells, harbor HCV viral RNA that replicates autonomously, and they express viral proteins. We treated cells that harbored a subgenomic replicon (#4-1, genotype 2a) [3,4] with the SERMs for 48 h and measured the amount of cellular replicon RNA by quantitative RT-PCR. Treatment with 10 μM of tamoxifen, raloxifene, or 3 μM of clomifene, inhibited HCV RNA compare to GAPDH RNA, although statistical significance was shown in only the inhibition of 10 μM of tamoxifen. ICI 182,780 did not show specific inhibition of HCV RNA (Fig. 3a).

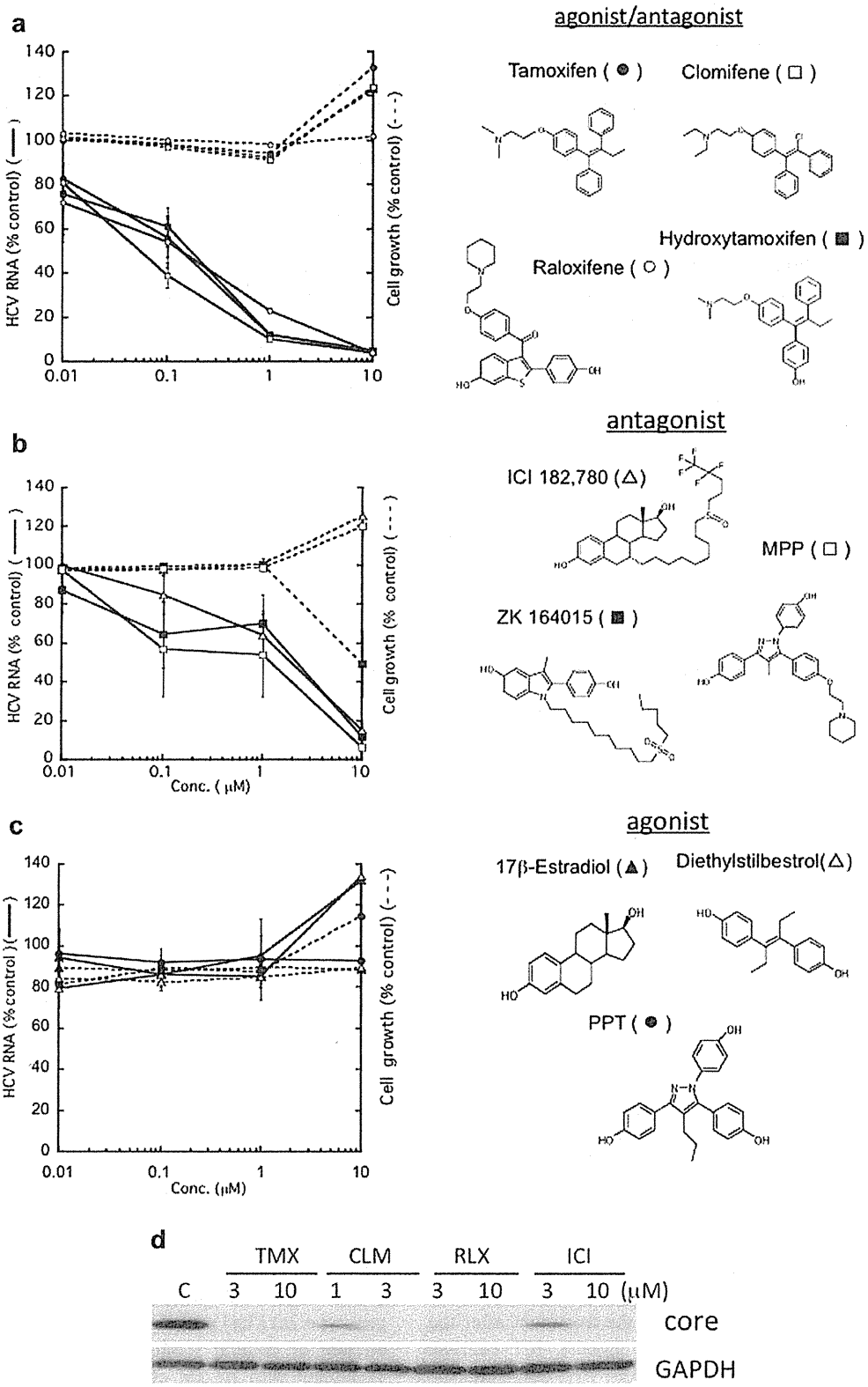

Fig. 1. Effects of SERMs on JFH-1 HCV RNA levels. a) Effects of tamoxifen, clomifene, and raloxifene. Huh 7.5.1 cells were infected with HCV JFH-1 (moi 0.01) in the presence of drugs and were incubated for 5 days. Drugs were added just before viral inoculation. HCV RNA in the medium was measured by tube-capture-RT-PCR [2]. Parallel cultures of cells without virus were analyzed using the MTT assay to detect the inhibition of cell growth due to drug exposure. Tamoxifen (closed circles), clomifene (open rectangles), hydroxytamoxifen (closed rectangles), and raloxifene (open circles). The percentages to control HCV RNA and